

ANALYSIS OF BEARING CAPACITY
USING DISCRETE ELEMENT METHOD

A THESIS SUBMITTED TO
THE GRADUATE SCHOOL OF NATURAL AND APPLIED SCIENCES
OF
MIDDLE EAST TECHNICAL UNIVERSITY

BY

ÖMER ARDIÇ

IN PARTIAL FULFILLMENT OF THE REQUIREMENTS
FOR
THE DEGREE OF MASTER OF SCIENCE
IN
CIVIL ENGINEERING

DECEMBER 2006

Approval of the Graduate School of Natural and Applied Sciences

Prof. Dr. Canan Özgen
Director

I certify that this thesis satisfies all the requirements as a thesis for the degree of Master of Science.

Prof. Dr. Güney Özcebe
Head of Department

This is to certify that we have read this thesis and that in our opinion it is fully adequate, in scope and quality, as a thesis for the degree of Master of Science.

Assoc. Prof. Dr. B. Sadık Bakır
Supervisor

Examining Committee Members

Prof. Dr. Erdal Çokça	(METU, CE)	_____
Assoc. Prof. Dr. B. Sadık Bakır	(METU, CE)	_____
Assoc. Prof. Dr. Ahmet Yakut	(METU, CE)	_____
Dr. A. Fikret Gürdil	(TEMELSU)	_____
Dr. M. Tolga Yılmaz	(METU, ES)	_____

I hereby declare that all information in this document has been obtained and presented in accordance with academic rules and ethical conduct. I also declare that, as required by these rules and conduct, I have fully cited and referenced all material and results that are not original to this work.

Name, Last name :

Signature :

ABSTRACT

ANALYSIS OF BEARING CAPACITY USING DISCRETE ELEMENT METHOD

Ardıç, Ömer

M.S., Department of Civil Engineering
Supervisor: Assoc. Prof. Dr. B. Sadık Bakır

December 2006, 89 pages

With the developments in computer technology, the numerical methods are used widely in geotechnical engineering. Finite element and finite difference are the most common methods used to simulate the behavior of soil and rock. Although the reliability of these methods are proven in several fields of application over the years, they are not equally satisfactory in every case and require sophisticated constitutive relations to model the discontinuous behavior of geomaterials since they assume the material is continuum or the location of discontinuum is predictable. The Discrete Element Method (DEM) has an intensive advantage to simulate discontinuity. This method is relatively new and still under development, yet it is estimated that it will replace of the continuum methods largely in geomechanics in the near future.

In this thesis, the theory and background of discrete element method are introduced, and its applicability in bearing capacity calculation of shallow foundations is investigated. The results obtained from discrete element simulation of bearing capacity are compared with finite element analysis and analytical methods. It is concluded that the DEM is a promising numerical analysis method but still have some shortcomings in geomechanical applications.

Keywords: Discrete Element Method, Particle Mechanics, Bearing Capacity

ÖZ

AYRIK ELEMANLAR YÖNTEMİ İLE TAŞIMA GÜCÜ ANALİZİ

Ardıç, Ömer

Yüksek Lisans, İnşaat Mühendisliği Bölümü
Tez Yöneticisi: Doç. Dr. B. Sadık Bakır

Aralık 2006, 89 sayfa

Bilgisayar teknolojisindeki gelişmelere bağlı olarak, sayısal yöntemlerin zemin mekaniğindeki kullanımı yaygınlaşmaya başlamıştır. Zeminin ve kayaçların davranışlarının benzetiminde sonlu elemanlar ve sonlu farklar yöntemleri yaygın olarak kullanılmaktadır. Birçok uygulama alanında güvenilirliği kanıtlanmış olmasına karşın bu yöntemler malzemeyi sürekli veya süreksizliklerin yerinin önceden bilindiği varsayımlarına dayandıkları için zeminlerin süreksizlik davranışlarını modellemekte her zaman başarılı olamamakta veya oldukça karmaşık yaklaşımlar gerektirmektedir. Ayrık Elemanlar Yöntemi süreksiz malzeme özelliğini modellemekte oldukça başarılıdır. Her ne kadar görece yeni ve gelişmekte olan bir yöntem olsa da, ileride zemin mekaniği problemlerinde süreklilik temelli yöntemlerin büyük ölçüde yerini alacağı düşünülmektedir.

Bu tezde, ayrık elemanlar yönteminin teorisi ve geçmişi incelemekte ve bu yöntemin sığ zeminlerdeki taşıma gücü hesaplarında kullanımı araştırılmaktadır. Ayrık elemanlar yöntemi ile yapılan taşıma gücü hesapları, sonlu elemanlar analizi ve analitik yöntemlerle karşılaştırılmıştır. Ayrık elemanlar yöntemi, zeminlerin sayısal analizlerinde ilerisi için umut veren eden bir yöntem olmasına karşın hala bazı sıkıntıları olduğu sonucuna varılmıştır.

Anahtar Kelimeler: Ayrık Elemanlar Yöntemi, Parçacık Mekaniği, Taşıma Gücü

ACKNOWLEDGMENTS

I would like to express my deepest gratitude to all who contributed to the preparation of this study.

First, I would like to thank my supervisor Assoc. Prof. Dr. B. S. Bakır for his guidance and recommendations. He truly motivated me to complete this study.

I am indebted to my company TEMELSU which played a very important role in my development. She provided time, environment and materials for this study.

I am also quite grateful to my wife Zeynep for her encouragement and support.

Last but not the least, I am indebted to DEM Solutions Ltd., especially Dr. J. Favier and Dr. C.J. Riley for their major contribution to this study by supplying major software and technical support.

TABLE OF CONTENTS

PLAGIARISM	iii
ABSTRACT	iv
ÖZ	v
ACKNOWLEDGMENTS.....	vi
TABLE OF CONTENTS	vii
CHAPTER	
1 INTRODUCTION.....	1
1.1 Discrete Element Method (DEM)	1
1.2 Fields of Application.....	6
1.3 Advantages and Disadvantages.....	15
1.4 Available Computer Programs.....	19
2 THEORY OF DISCRETE ELEMENT METHOD.....	21
2.1 Fundamentals of Discrete Element Method.....	21
2.1.1 General	21
2.1.2 Calculation Scheme.....	22
2.1.3 Velocity Issue.....	24
2.1.4 Issues of Stress and Strain.....	26
2.1.5 Parameter Selection.....	26
2.2 Theory of Motion and Position Calculation.....	27
2.3 Contact Constitutive Relations.....	29
2.3.1 Contact – Stiffness Models	30
2.3.2 Contact – Yield Model.....	33
2.3.3 Damping models	34
2.4 Stable Time Step	38
2.5 Other Forms of DEM	40

3 APPLICATION OF DEM ON BEARING CAPACITY PROBLEMS	43
3.1 Introducing the DEM Software EDEM™	43
3.1.1 General	43
3.1.2 Element types	43
3.1.3 Computation technique	44
3.1.4 Contact models	45
3.1.5 Post-Processor	46
3.2 Analysis Procedure	46
3.3 Calibration Runs	49
3.3.1 Isotropic Compression Test Simulation	49
3.3.2 Direct Shear Test Simulation	55
3.4 Bearing Capacity Calculation Models	60
3.4.1 Bearing Capacity From Analytical Methods	61
3.4.2 Numerical Analysis of Bearing Capacity by FEM	63
3.4.3 Numerical Analysis of Bearing Capacity by DEM	66
4 DISCUSSION OF RESULTS AND CONCLUSIONS	72
REFERENCES	75

LIST OF TABLES

TABLES

Table 3.1 Micro-mechanical parameters selected for analyses.....	48
Table 3.2 Properties of geometric model	48
Table 3.3 Results from isotropic compression test	53
Table 3.4 Calculation of macro-elastic parameters.....	54
Table 3.5 List of N_γ term for the bearing capacity formulations	62
Table 3.6 Model parameters for FEM analysis of bearing capacity	63

LIST OF FIGURES

FIGURES

Figure 1.1 Observation scale in the classification of numerical modeling techniques of materials (D'Addetta, 2004).....	2
Figure 1.2 Simulation of an hourglass by DEM	3
Figure 1.3 Simulation of failure zones under a footing by stack of rods (Lambe and Whitman, 1979).	4
Figure 1.4 Simulation of failure of braced excavation by rods (Lambe and Whitman, 1979).	5
Figure 1.5 Numerical analysis of impact (Magnier and Donze, 1998).....	8
Figure 1.6 Numerical analysis of vertical screw conveyor (Shimizu and Cundall, 2001)	9
Figure 1.7 DEM analysis of unconfined compression and tension test of concrete (Hentz et al, 2002).....	10
Figure 1.8 Formation of crushable soil assembly from bonded agglomerates (Cheng et al, 2003)	11
Figure 1.9 Numerical simulation of deep penetration by DEM (Jiang at al., 2005).....	12
Figure 1.10 Simulation of triaxial test for parameter calibration (Maynar and Rodriguez, 2005)	13
Figure 1.11 Earth pressure balance tunnel simulation by DEM (Maynar and Rodriguez, 2005)	13
Figure 1.12 Numerical analysis of concrete faced rockfill dam by DEM (Deluzarche and Cambou, 2006).....	14
Figure 2.1 Calculation circle of Discrete Element Method.....	23
Figure 2.2 Illustration of the effect of velocity (rate of loading) (ABAQUS Documentation, 2004)	25
Figure 2.3 Effect of velocity to the failure mechanism of the backfill behind a retaining structure (D'Addetta, 2004).....	25

Figure 2.4 Illustration of viscous damping between particles (Itasca, 2006).....	35
Figure 2.5 Example of multi-element clusters (Favier, 1999).	41
Figure 3.1 Illustration of EDEM™ user interface.....	44
Figure 3.2 Generated input model.....	49
Figure 3.3 Isotropic compression test model	51
Figure 3.4 Contact overlap distance at the final stage of isotropic compression test.....	51
Figure 3.5 Measured forces during isotropic compression test simulation.....	52
Figure 3.6 Variation of stresses in isotropic compression test.....	54
Figure 3.7 Variation of normal stress on shear plane.....	57
Figure 3.8 Graphics of shear to normal force ratio during direct shear test.....	58
Figure 3.9 Direct shear test simulation	59
Figure 3.10 Bearing capacity model dimensions	60
Figure 3.11 Phase ² model of bearing capacity analysis	64
Figure 3.12 Indication of major principal stress on deformed shape of the FEM model at 0.15 m settlement of footing (True scale at $\psi=0^\circ$)	64
Figure 3.13 Displacement versus vertical stress diagram from FEM analysis	65
Figure 3.14 The Progress of bearing capacity failure in time	66
Figure 3.15 Displacement versus footing pressure diagram from DEM analysis.....	69
Figure 3.16 Comparison of bearing capacity calculations	70
Figure 3.17 Comparison of deformed shape of FEM and DEM as of 0.15 m settlement.....	71

CHAPTER 1

INTRODUCTION

1.1 Discrete Element Method (DEM)

Numerical analyses are being used increasingly by the engineers parallel to the developments in the computer technologies. By means of numerical analysis programs, engineering problems can be solved more precisely and the complex, sophisticated projects can be handled with greater confidence. Finite Element Method (FEM), Finite Difference Method (FDM) and Boundary Element Method (BEM) are the examples of numerical analysis methods that are widely applied presently. The common property of these methods is that the material is idealized as a continuum. Although it is possible to introduce a discontinuity if its location is known beforehand, they can not simulate the distinct property of discontinuity as in the case of geomaterials.

The idealization of continuum and the related terms such as stress and strain are commonly used in engineering. As far as the continuum assumption is valid throughout the analysis and relatively simple constitutive relations are applicable, FEM is very effective, proven and widely used at present. Also a variety of commercial computer programs that are built on this method are available in the market. The continuum based methods, especially FEM, are commonly used in geotechnical applications as well, in order to simulate the behavior of soil and rock.

The finite element method uses constitutive (stress-strain) relations to simulate the behavior of continuum materials. The constitutive relations used to model the continuum range from the simple linear elastic to elasto-plastic models with multiple yield surfaces, non-associated or dilative flow rules and general hardening/softening rules. Depending on the circumstances extremely sophisticated constitutive relations can be required for geomaterials since their response can be rather complex under certain conditions. There exist various constitutive relations

proposed for geomechanical applications depending on the soil type and drainage circumstances. Additionally, increase in complexity of constitutive relation increases the number of parameters, some of which do not have clear physical meanings. It is sometimes quite difficult to measure these parameters.

In order to overcome the shortcomings of the continuum approach, Discrete Element Method or as also called Distinct Element Method (DEM) has been developed. Discrete element method models the materials with separate particles. This method is suitable not only to simulate the behavior of geomaterials but also the behavior of any particulate matter like powders or grains. Figure 1.1 shows the range of applicability of DEM compared to the other numerical methods.

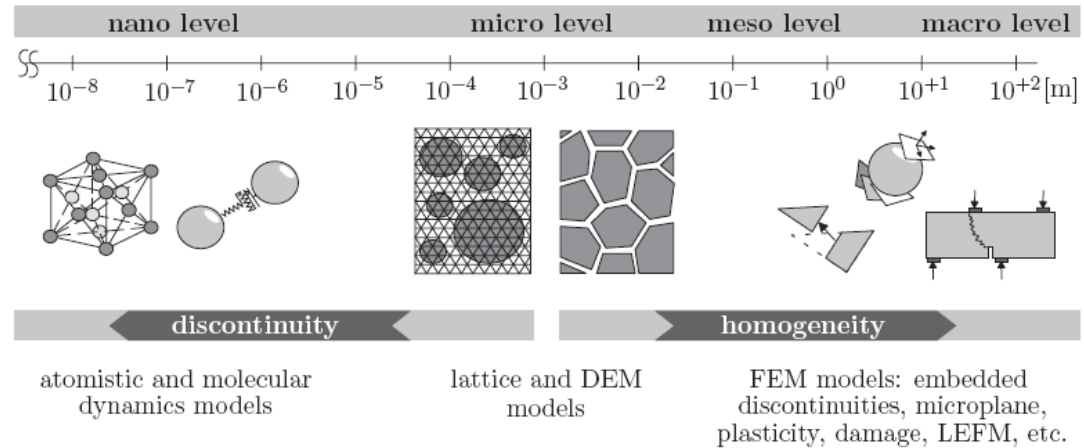


Figure 1.1 Observation scale in the classification of numerical modeling techniques of materials (D'Addetta, 2004)

Soil and rock behave in a rather complicated manner due to their distinct properties. It is sometimes necessary to model the discontinuum behavior of these materials as in the case of soil liquefaction or in simulating the post-failure mechanism of slopes. Separation may take place on the slip surface or elsewhere with the sliding mass following failure and it can affect the reliability of analyses. Such a model can be properly handled by DEM simulations.

Mohammadi (2003) draws the attention to the simulation of flow of sand in an hourglass. The sand hourglass which is used for centuries to measure the time could not be modeled accurately on the computer by even the enhanced numerical methods such as FEM until recently. Simulation of this problem, however, is rather straightforward with DEM approach and the results are quite accurate although too much calculation time may be required for the current computer technology. An hourglass simulation with around 500 particles is modeled for illustrative purposes (Figure 1.2). The simulation is terminated at 0.7 second due to blocking.

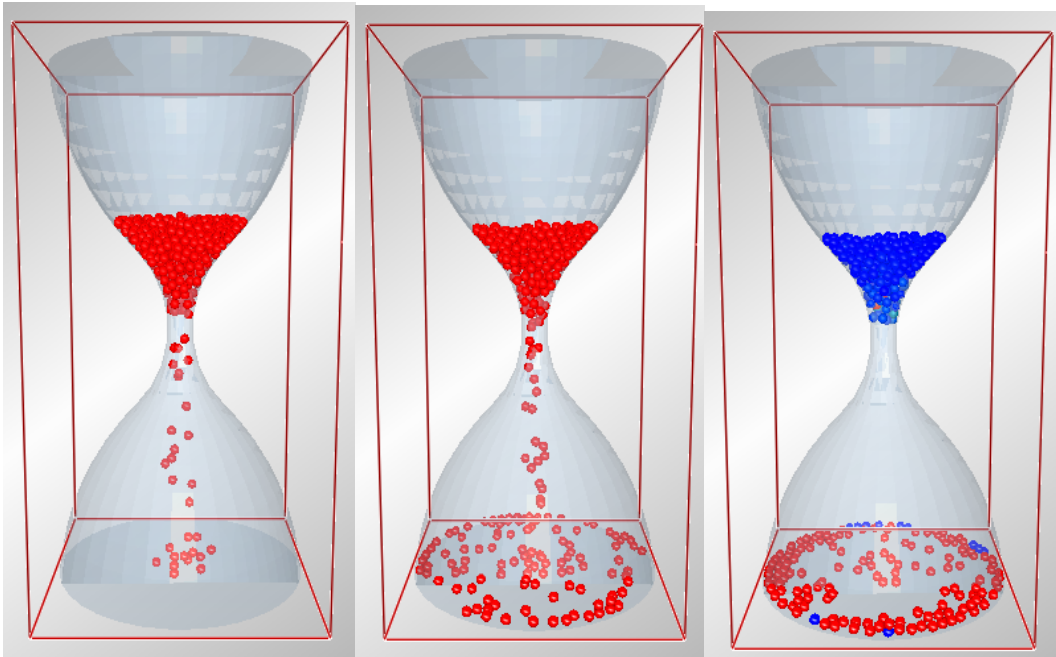


Figure 1.2 Simulation of an hourglass by DEM

Author is motivated to work on this subject due to laboratory simulations performed by Lambe and Whitman (1979) in order to investigate the failure mechanism of shallow foundation and braced cuts by using stack of rods to represent the granular soil media. The philosophy of discrete element model can not be summarized better than those studies, the relevant failure mechanism of which are given in Figure 1.3 and Figure 1.4, respectively.

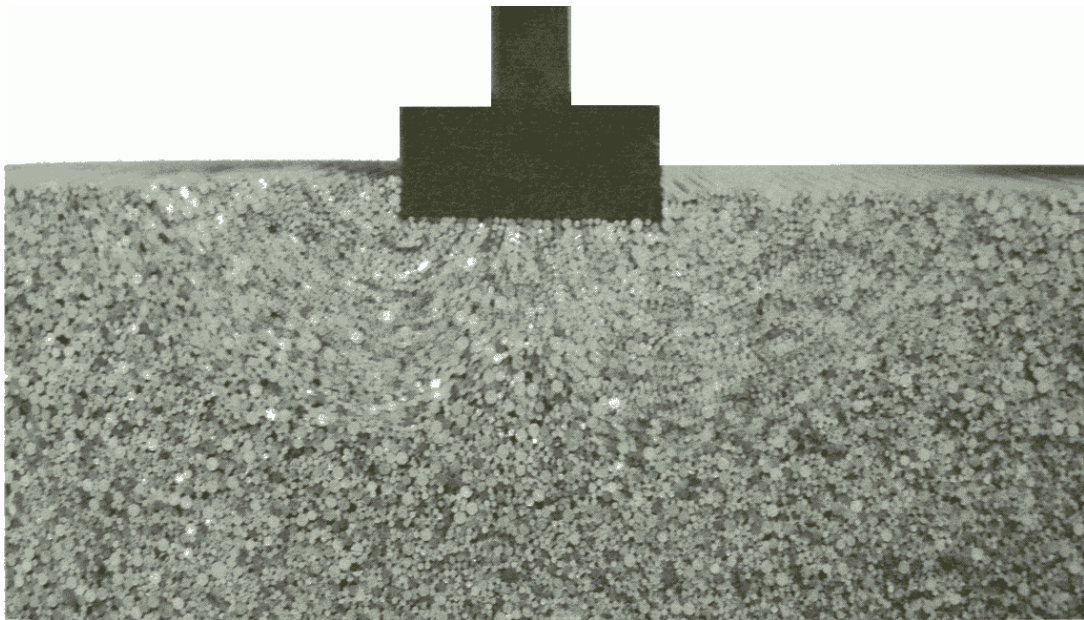


Figure 1.3 Simulation of failure zones under a footing by stack of rods (Lambe and Whitman, 1979)

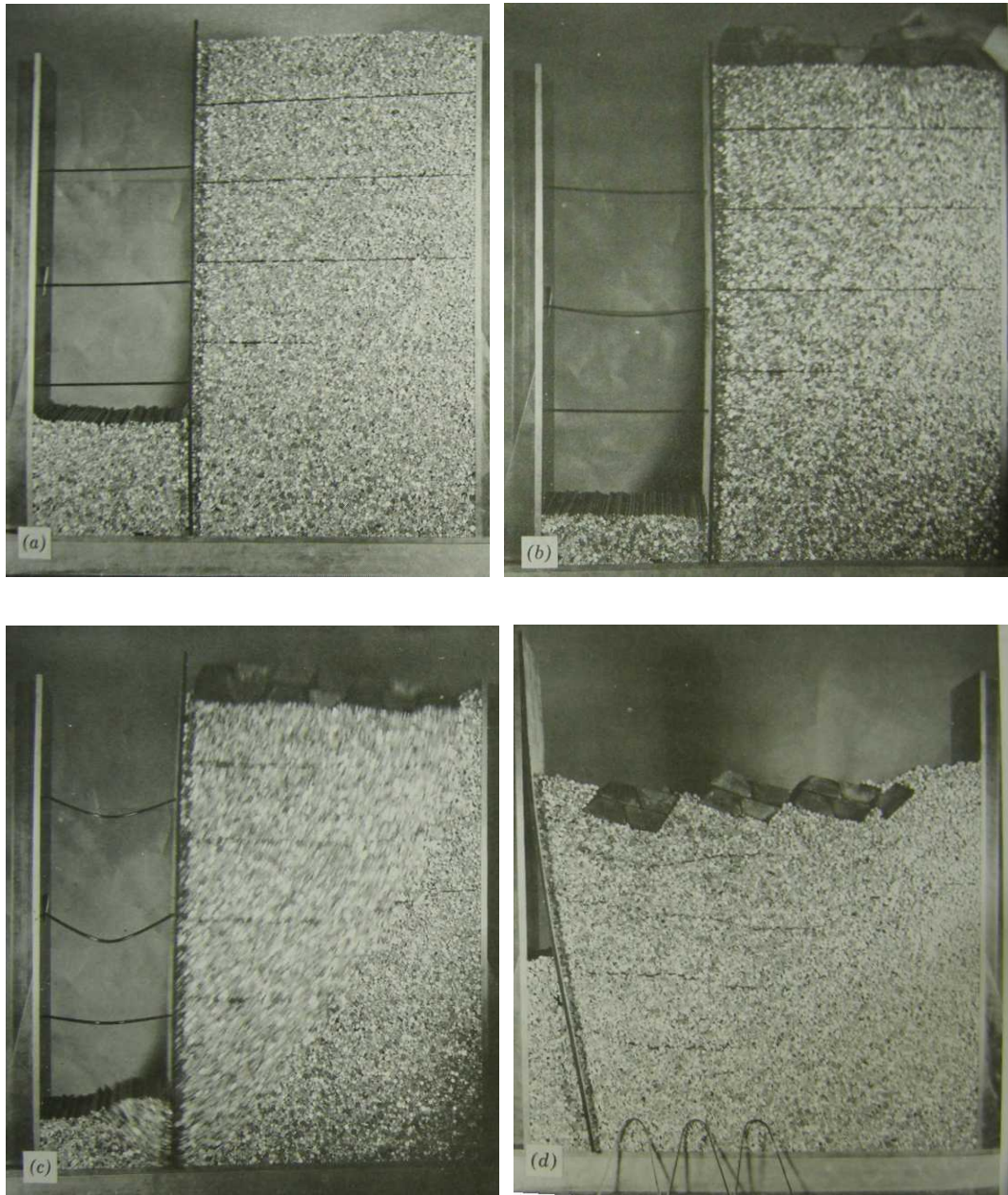


Figure 1.4 Simulation of failure of braced excavation by rods (Lambe and Whitman, 1979)

It is acknowledged that the studies on the discontinuum mechanics leading to DEM have been started by Cundall (1971). The formulation of DEM for modeling the distinct behavior of granular soils was first introduced by Cundall and Strack (1979). They claim that the granular materials can be simulated by disks (in 2 dimensions) or spheres (in 3 dimensions) which move according to Newton's second law of motion and interact by contact constitutive laws.

DEM is relatively new and still under development. Hence, unlike FEM, it is not investigated yet thoroughly in applications. In today's advanced finite element programs, it is possible to define a discontinuity by contact formulations and stresses can be transferred between contact surfaces by suitable contact constitutive laws. However, the philosophy behind DEM is much simpler than other numerical analysis methods and is certainly promising for the geotechnical engineering area. According to Cundall (2001) who is presumably the originator of DEM, this method will be the alternative for any continuum based method in geomechanics in near future.

1.2 Fields of Application

Unlike the FEM or FDM, DEM was devised originally for geomechanics. The other numerical methods which are based on continuum idealization are developed for the elastic or perfectly plastic frictionless materials having nearly linear stress-strain relation. The metals such as steel perfectly fit this definition.

FEM is also applicable to the numerical analysis of geotechnical problems by introducing special constitutive relations. There exist plenty commercial FEM programs specially produced for geomechanical applications. Correspondingly, most of the general purpose FEM packages comprise the geomechanical constitutive relations as well. Accordingly, the FEM is the ultimate method in the numerical analysis in geomechanics at present.

Theoretically speaking, it is possible to use DEM alternatively in the geomechanical problems where the FEM can be used. Furthermore, modeling of continuum by DEM is also possible by particular contact constitutive relations (Section 2.3). For

instance, the continuum can be modeled by discrete particles in the problems where the continuum and discontinuum are needed to be modeled simultaneously like as in the case of soil-structure interaction analysis. However, the best solution may be to employ FEM-DEM coupled methods in order to model such problems.

Practically, due to the disadvantages of DEM discussed in Section 1.3, the fields of application are limited as of present. Increased interest in DEM and increase in computer processor speeds will lead to increase in the quality and quantity of available DEM based computer programs. Mohammadi (2003) listed the current research on discontinuum mechanics as follows:

- Geomechanical applications
- Granular materials (like powders, grains, etc.)
- Impact analysis (progressive fracturing)
- Particulate flow
- Computer graphics

Since the large scale problems require excessive calculation times, the example simulations performed by DEM are generally small scale. Obviously, the smallest scale simulations in geomechanics are the laboratory tests. It is possible to simulate triaxial, biaxial, unconfined compression or shear box tests through DEM.

Some interesting studies reviewed by the author are illustrated in the rest of this section.

The numerical analysis of impact performed by Magnier and Donze (1998) is an excellent study showing the efficiency of DEM in progressive fracturing. They investigated the failure behavior of unreinforced and reinforced beams during the impact of a spherical nose shaped missile (Figure 1.5).

Shimizu and Cundall (2001) conducted 3-dimensional DEM analysis in order to examine the performance of screw conveyors and the results obtained from this study was compared with the previous studies and empirical solutions (Figure 1.6).

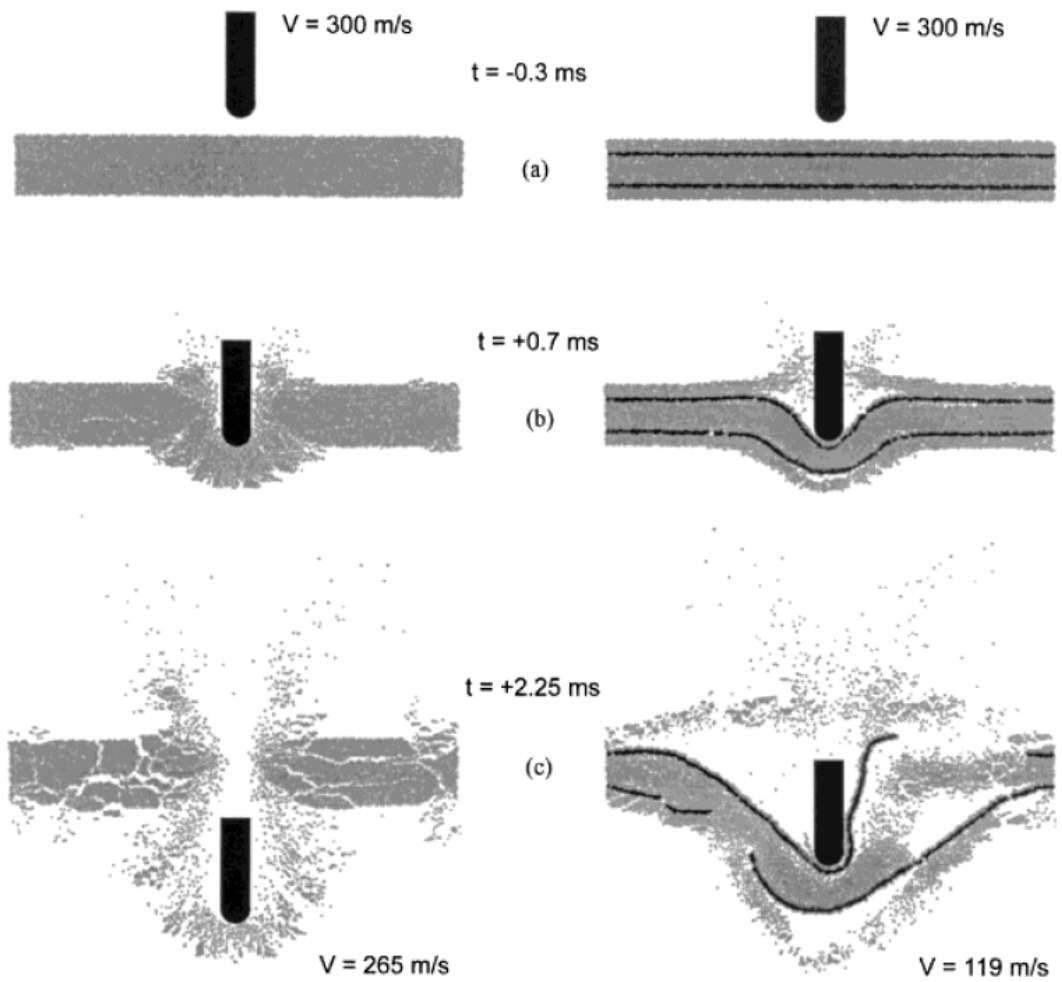


Figure 1.5 Numerical analysis of impact (Magnier and Donze, 1998)

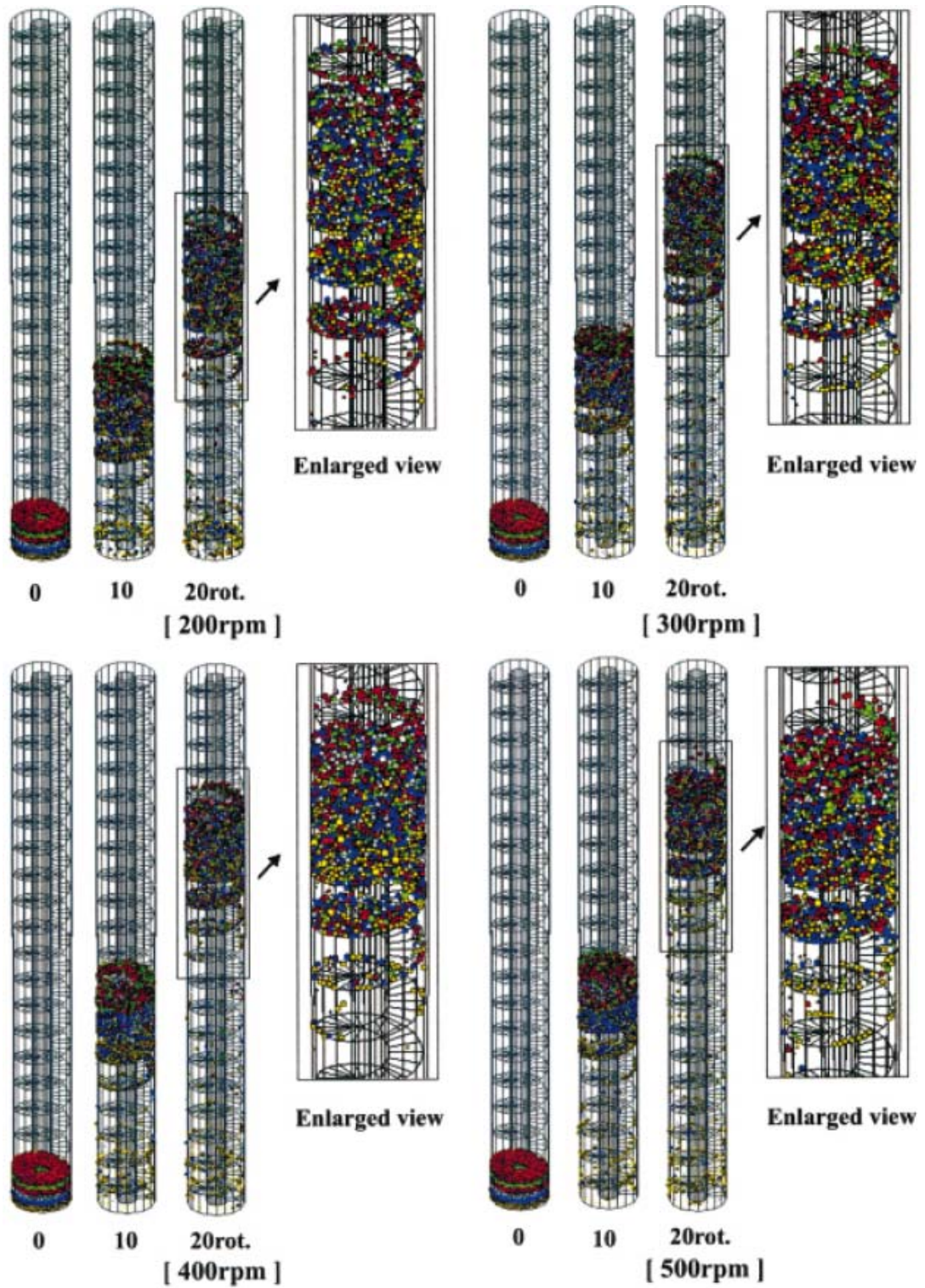


Figure 1.6 Numerical analysis of vertical screw conveyor (Shimizu and Cundall, 2001)

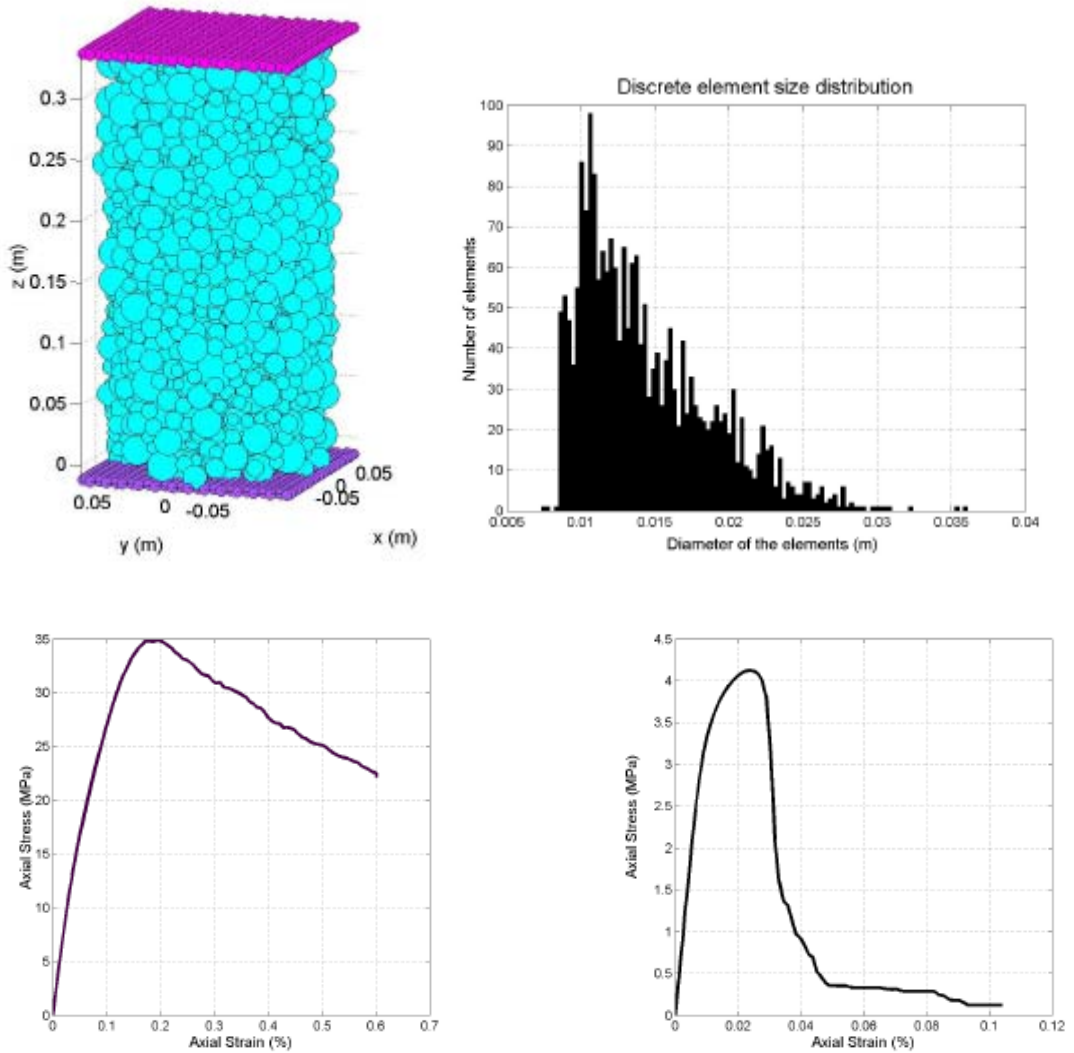


Figure 1.7 DEM analysis of unconfined compression and tension test of concrete (Hentz et al, 2002)

In order to investigate the fracture and failure mechanism of concrete, Hentz et al (2002) performed DEM simulations of unconfined compression and tension tests. They examined the constitutive behavior of concrete and elastic-inelastic deformations (Figure 1.7).

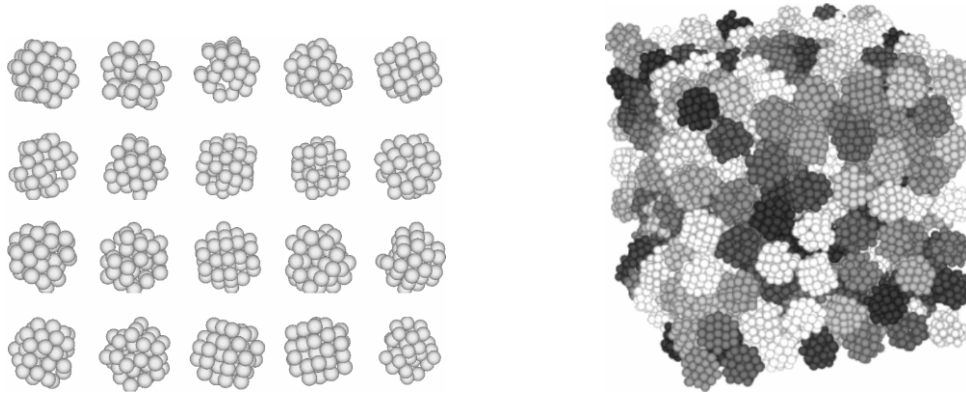


Figure 1.8 Formation of crushable soil assembly from bonded agglomerates (Cheng et al, 2003)

DEM simulation of crushable soil illustrated by Cheng et al (2003) is an interesting study. In this study, bonded agglomerates representing the single crushable grain were formed (Figure 1.8). Then, model was generated by using these agglomerates and some tests were performed.

Denish and Sitharam (2003) studied on the drained and undrained behavior of soil under cyclic loading by DEM conducted triaxial test. This is an interesting study as it shows the modeling of liquefaction by DEM.

Jiang et al (2005) presented a paper on the numerical study on deep penetration mechanisms in granular materials with the focus on the effect of soil–penetrometer interface friction. They investigated the soil displacement path near the penetrometer and effect of interface friction on the actual penetration mechanism (Figure 1.9).

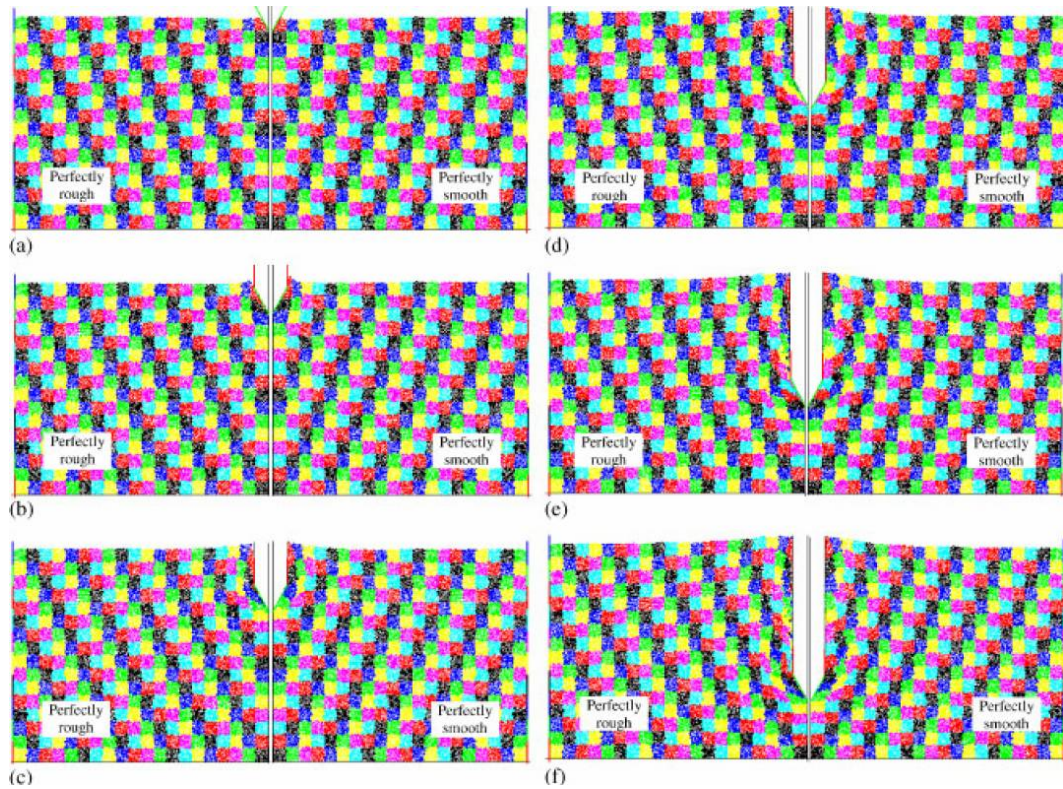


Figure 1.9 Numerical simulation of deep penetration by DEM (Jiang at al., 2005)

Maynar and Rodriguez (2005) were presented a numerical study on the DEM simulation of earth pressure balance (EPB) tunnel excavation. The purpose of their study was to analyze the technical requirements of the shields (thrust and torque) needed to excavate the tunnel. They also investigated the tunnel face stability problem. In the first phase of study, they made calibration runs by triaxial test simulations (Figure 1.10). Then, a tunnel excavation model was created and analyzed. (Figure 1.11)

Perhaps the most challenging and comprehensive DEM study reviewed by the author is the one performed by Deluzarche and Cambou (2006). The numerical analysis of a concrete faced rockfill dam constructed at 1950 was investigated in this study (Figure 1.12).

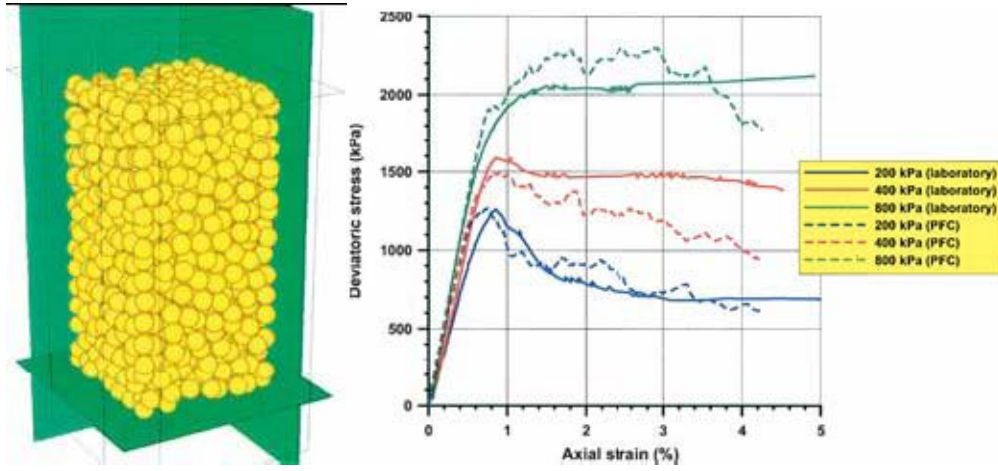


Figure 1.10 Simulation of triaxial test for parameter calibration (Maynar and Rodriguez, 2005)

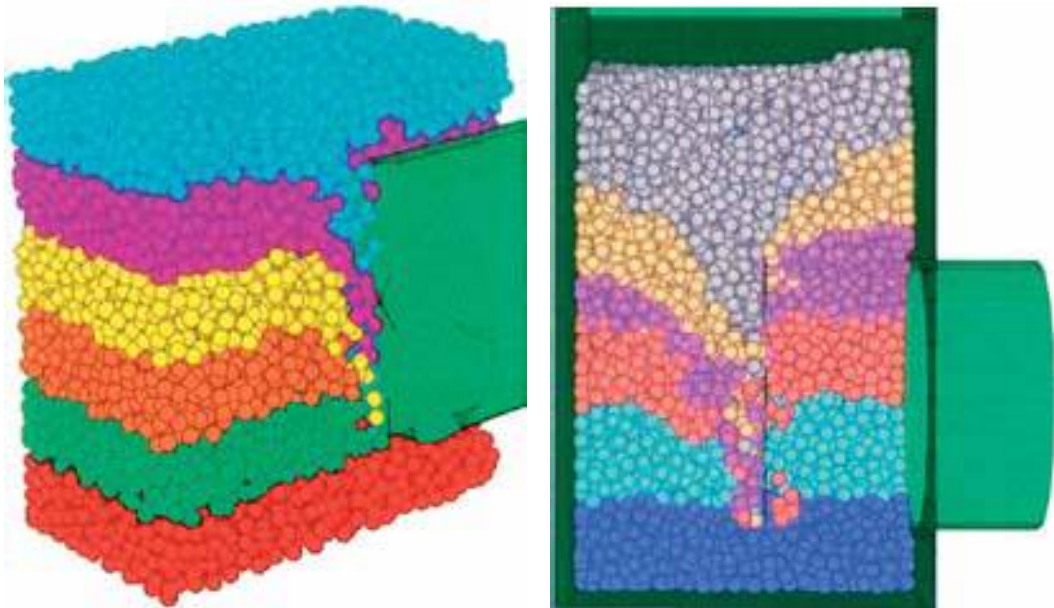


Figure 1.11 Earth pressure balance tunnel simulation by DEM (Maynar and Rodriguez, 2005)

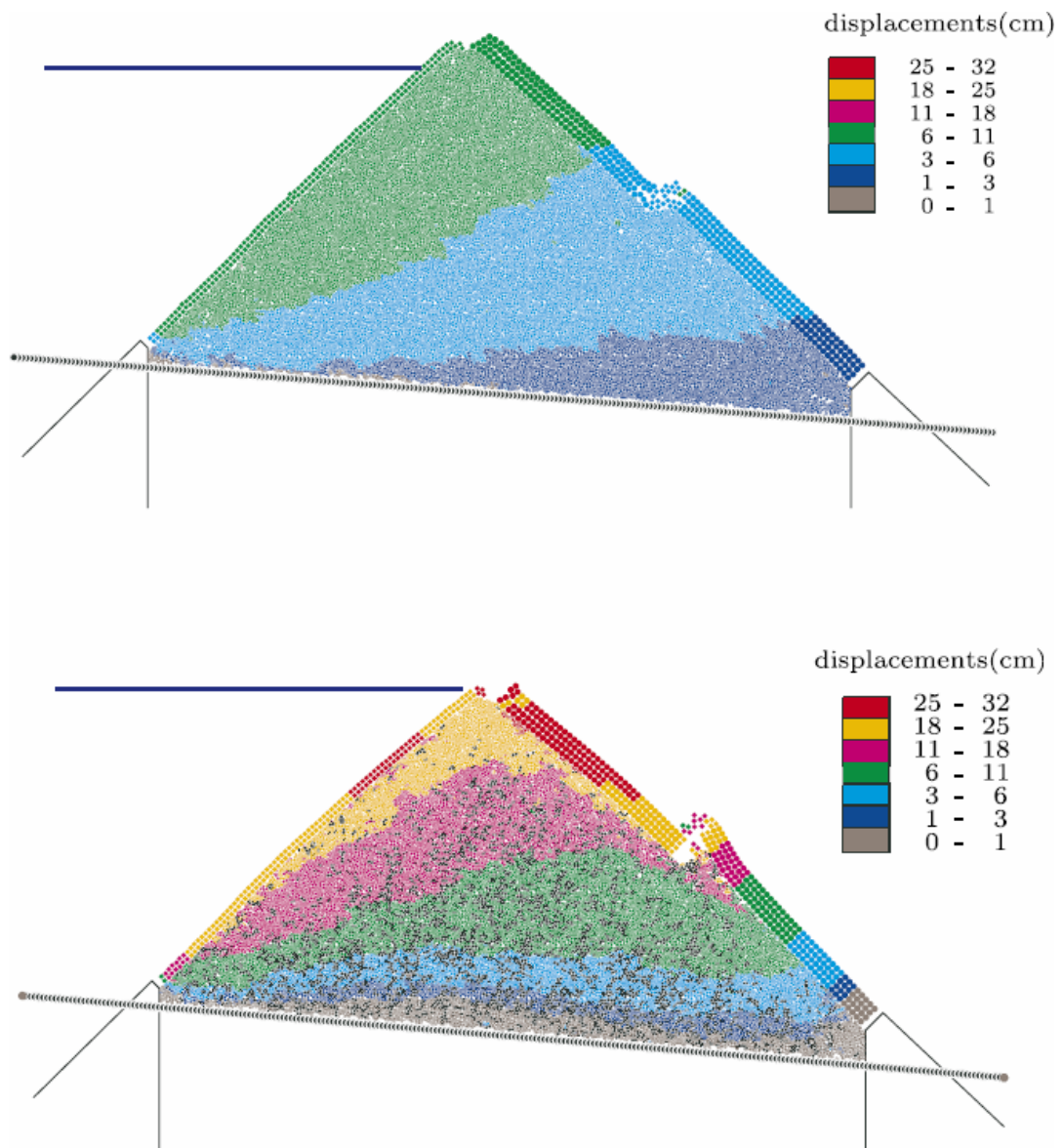


Figure 1.12 Numerical analysis of concrete faced rockfill dam by DEM (Deluzarche and Cambou, 2006)

1.3 Advantages and Disadvantages

Advantages and disadvantages of a particular method can be illustrated by comparing its performance to the alternative methods in specific fields of application. Clearly, FEM is the most commonly used and comprehensive numerical analysis method in the field of geotechnical engineering. Therefore, the FEM is the natural reference to evaluate the advantages and disadvantages of the DEM. Although this study primarily concentrates on geomechanics, an overall comparison may be useful to display the general qualities that are valid usually in other disciplines as well. Indeed, there exist certain fields in which a particular method has unrivalled advantages and hence shall not be replaced by another one. These fields are also discussed in this section.

Obviously, the theory behind the FEM is solid and verified in numerous fields of application. On the other hand, DEM is a relatively new method and still under development. The available literature on the theory and applications of the DEM are rather limited at present. Since it requires extremely high computation time, the validation of this method in geomechanics is restricted to small applications like laboratory tests as yet (Cundall, 2001).

The terms and parameters akin to continuum mechanics are universally used in engineering. Since the FEM is used for several decades, there exist standardized laboratory and field tests to measure the parameters relevant to the continuum mechanics and hence to the FEM such as Young's modulus, Poisson's ratio, etc. However, granular based laboratory tests are not common. Therefore, a calibration stage is normally required in discrete modeling in order to match the micro and macro scale parameters. In the simulations of geomaterials, this situation remains as a standard difficulty in the DEM, whereas, the measurements of some other parameters required by continuum constitutive relations may not always be practical (see the paragraph below).

In the FEM, the material behavior is defined by a relationship between the stress and strain which is known as the constitutive equation. For the non-frictional materials like metals, this relation is relatively simple and requires few parameters

with clear physical meanings. All FEM based programs provide the linear constitutive model as standard. Additionally, Huber-von Mises constitutive relation is widely used to simulate the plasticity of frictionless materials. However, there exist numerous constitutive relations for frictional materials with different approximations and assumptions. Their behavior and strength are different in tension and compression. The simulation of this phenomenon requires intricate constitutive relations. Mohr-Coulomb, Drucker-Prager, Matsuoka-Nakai, Lade-Duncan, Hoek-Brown, Cam Clay are the most common constitutive relations for geomaterials. The number of required parameters increases with increasing complexity of the model and sometimes these parameters do not have clear physical meanings (Alonso-Marroquin, 2004). Accordingly, it may be difficult to access some of these parameters. On the other hand, behavior of the particles is governed by contact constitutive relations in DEM. There exist few contact constitutive relations and they require fewer parameters with relatively more clear meanings.

In the case of FEM, the calculation time is directly associated with the number of degrees of freedom of the model which depend on the size of the solution mesh. The required size of the mesh is generally specific to the problem. Increasing the mesh density in the region of interest and stress concentration areas and decreasing towards the boundaries is accepted as a good meshing technique. Some of the enhanced FEM based programs have adaptive meshing capability in order to adjust the mesh density automatically. Generally speaking, the reliability of the results depends on the meshing at great degree. Similarly in the DEM, the number of particles defines the required duration of the calculation. Ideally, the particle sizes are required to be similar or proportional to the actual grain size in the simulation of granular materials. However, since it is not either practical or possible to model every particle, a particle scaling process is necessary and this may again require additional calibrations of the model. For the modeling of continuum in the DEM, the scaling of the bonded particles is similar to the FEM. That is to say, increase in particle density leads to increase in solution accuracy.

The computation time is a critical factor in the computer based numerical analyses. The effectiveness of the calculation process is actually dependent on the speed of

the computer processor. As far as the dimensions of geotechnical problems are considered, the current computer technology is quite appropriate for the simulation of static problems by FEM. Dynamic simulation of highly plastic materials requires computation capacity that are still excessive for average personal computers. However, parallel processing techniques in FEM based programs are available to utilize the powers of a number of processors simultaneously. Conversely, the DEM uses explicit finite difference solution scheme. Therefore, it is fully dynamic. Due to the fact that the disturbance should not propagate to the neighboring particles and the accelerations should be constant in a single time step, stable time step must be very small (see Section 2.4). Additionally, the necessity of excessive number of particles substantially increases the computation time. The simulation of practical geomechanical problems is not efficient considering the current computer speeds.

One of the major disadvantages of the DEM is the difficulty of formation of model geometry. Either the geometrical forms can be filled by particles or particles have to be placed one by one. In the former, the user control on the particle distribution is quite limited. There is a full control in the latter case but it can be a challenging task even with a specially generated code. In either case, the geometry can differ when the forces like gravity are applied to achieve the initial stress conditions before starting to analysis. In the FEM based computer programs, however, the definition of model geometry is relatively simple. Extremely capable mesh building engines are available to form very complex geometries even in three dimensions.

Presently numerous FEM based computer programs are available in the market. The quality and quantity of these softwares are increasing parallel to the developments in computer technology. There exist FEM based programs developed for the specific applications besides the general purpose programs. Whereas, only few DEM based programs are available since this method is relatively new and the required computational effort is excessive as of present.

The FEM is widely used in structural analysis as well. For that purpose, FEM software packages contain truss, beam, shell, membrane and similar elements, and

plane-stress solution scheme is available. The DEM, however, can only simulate solid elements. Two-dimensional simplification can only be plane-strain.

Since the DEM can handle complete detachment at any arbitrary location, it is very effective in simulation of particulate mechanics and fracture mechanisms. It is not possible to model detachment in the FEM unless the location of separation is known as anticipated beforehand. Therefore, DEM has certain advantages in areas where FEM has limitations.

Since DEM is fully dynamic, visualization of the results can be very instructive to clearly realize the mechanisms. Sitharam (2000) stated that the major advantages of DEM may be having chance of observing any particular details during the simulation. Thus, it is quite efficient for instructional and demonstrative purposes.

Under the lights of above comparison between DEM and FEM, advantages and disadvantages of DEM are summarized in the following:

Advantages:

- Contrary to the continuum approach, does not require sophisticated constitutive relations in geomechanical applications,
- Can realistically simulate the distinct behavior of granular materials,
- Requires relatively less parameters with clear physical meanings to define the material behavior such as contact stiffness and friction coefficient,
- Effective to investigate the particle based mechanisms, fracture mechanics, dynamic, large displacement and/or large strain problems (such as post-failure mechanisms), soil-structure interaction, etc.
- Efficient in visual recognition of problems due to its fully dynamic nature.

Disadvantages:

- Requires excessive computational time, thus it is not practical to simulate large problems currently,
- Requires calibration studies for determination of material properties,
- Poses difficulties in forming the geometries,

- There exist relatively few computer programs available on DEM in the market presently.

1.4 Available Computer Programs

Presently, there are several programs in the market which are capable of modeling discontinuum. However, there are few DEM programs available as yet. Cundall and Hart (1992) proposed that DEM program should have the following features:

- Allows finite displacements and rotations of discrete bodies, including complete detachment,
- Recognizes new contacts automatically as the calculation proceeds.

The first DEM programs are the Fortran coded “Ball” and “Trubal” developed by Cundall in 1979 and 1980, respectively. The formulations used in these programs are given by Cundall and Strack (1979).

Ball is a two dimensional program and simulates the particles as disks (or cylinders). Trubal, on the other hand, is a three dimensional code with spherical particles. Trubal was open-source and distributed freely for about 15 years and used extensively in research in the development of DEM. Also, it is the basis of today’s commercial DEM programs. Both of these programs are commercial presently. “Ball” and “Trubal” were further developed by Itasca Consulting Group Inc. and Cundall and named as PFC^{2D} (Particle Flow Code in Two Dimensions) and PFC^{3D} (Particle Flow Code in Three Dimensions).

Another program based on the dynamics of spherical particles in three dimensions is SDEC (Spherical Discrete Element Code) developed by F. V. Donze. This code has been used to treat geomechanical problems in both quasi-static and dynamic applications, especially in simulation of laboratory tests. SDEC is not distributed anymore but Ph.D. students O. Galizzi and J. Kozicki have included the codes of SDEC in their research project named YADE (Yet Another Dynamic Engine).

YADE is a free software distributed by GNU/GPL † and is under development with beta version being recently available. The developers of YADE aim to make it DEM-FEM coupled software but, in its current form it is far from being a professional program. Unless specific codes are provided to the program, one can only view the example projects. Its graphical platform is quite useful and theoretical background is solid. But user interface, pre and post processors need to be developed further.

There are other softwares available in the market. They are not thoroughly reviewed by author. Some of them are listed below:

- MIMES: A program developed in the Massachusetts Institute of Technology Department of Civil and Environmental Engineering with the contribution of J. R. Williams.
- PASSAGE/DEM: Commercial program developed by Technalysis Inc. It appears to be a professional program but the demo/trial version could not be viewed.
- ELFEN: Commercial DEM-FEM hybrid software developed by Rockfield Software Ltd. They do not provide demo/trial version of the software even for academic purposes.

Finally, maybe the best DEM software reviewed by the author is EDEM™ which is developed and distributed by DEM Solutions Ltd. It is very user friendly and has an excellent user interface. DEM Solutions Ltd. supports academic studies by supplying time limited free and discounted academic licenses. DEM Solutions Ltd. also supported the present thesis by supplying the fully functional program for a period of three months. EDEM™ is used in the entire discrete element simulations studied in this thesis and the detailed information on the theory and background of the program is given in Section 3.1

† The GNU system is a complete UNIX like operating system often referred as “Linux”. GNU is a recursive acronym for “GNU is Not UNIX”. The computer applications distributed with GNU/GPL (General Public License) are open source code and can be redistributed freely. It is possible to use a portion or complete source code of such softwares to develop new free programs.

CHAPTER 2

THEORY OF DISCRETE ELEMENT METHOD

2.1 Fundamentals of Discrete Element Method

2.1.1 General

Formulation of DEM requires a consideration of a number of concepts. These concepts can be classified according to the following aspects:

- Body or particle shape (disk, sphere, ellipsoid, polygonal etc.)
- Deformability of body or particle (rigid or deformable)
- Deformability of contact (rigid or deformable)
- Equation of motion (original time history or transformed, modal equations of motion)

The theory of DEM presented in this thesis is based on the study of Cundall and Strack (1979) † and particularly on the disk (in two dimensions) or spherical (in three dimensions) shaped rigid (undeformable) particles with deformable contact formulation. Particles move according to Newton's second law of motion in real time. The computer program EDEM™ is also based on this theory. The other forms of DEM and the influence of different particle shapes are discussed in Section 2.5.

The theory of discrete element method is in general much simpler than the alternative numerical analysis methods. This is because the particles in DEM

† In this study, they named this method as Distinct Element Method. Later, Cundall and Hart (1992) claimed that “the term Distinct Element Method had been coined to refer the particular discrete element scheme that uses deformable contacts and explicit, time-domain solution of the original equations of motion (not the transformed, modal equations)” in the paper where they studied the different forms of discrete element method.

displace and interact according to simple physical laws. This is also why the parameters required in this method have clear physical meanings although it may sometimes be difficult to assess them properly. The simulation of billiard balls is a good example to illustrate the parameters such as the stiffness of contact or damping coefficients that can be determined and fine tuned after several model studies. Actually, there are computer games and simulations modeling the motion of particles that also use simple forms of DEM.

2.1.2 Calculation Scheme

In the DEM, particles obey the Newton's second law of motion. It is a completely explicit dynamic time history analysis. Accordingly, if the forces acting on a particle are known at a specific time, its velocity, displacement and consequently the position can be calculated. This concept forms the basis of DEM approach.

Forces and moments acting on each particle in a system stem from external forces like gravity or contact reactions. It is obvious that a discontinuous medium is distinguished from a continuous one by the existence of contacts. The formulation which yields contact forces due to the deformation at contacts is referred as "contact constitutive relation" that is of critical importance in the discrete element formulation.

The contact detection algorithm is the most challenging part of discrete element programs. The computation time is directly dependent on this algorithm. If the contact existence is detected by investigating the position of each particle in the system, the amount of calculation time necessary to identify the contact points is proportional to the square of the number of particles in the system in each step. If ten thousand particles are considered for 1×10^{-5} s time-steps, the simulation with duration of 10 s requires 1×10^{14} contact detection iterations. If polyhedral particles are used instead of spherical ones, computational demand grows beyond imagination. Fortunately, there are more efficient contact detection algorithms which reduce the number of contact detection iterations and the investigations on

this subject are still ongoing (e.g. Nezami, Hashash, Zhao and Ghaboussi, 2004 and 2006)

The calculation scheme in DEM can be generalized as follows: Displacements can be calculated for a time step by the Newton's second law of motion. Then the location of each particle is determined. The existence of contacts is searched by contact detection algorithm and relative position of each particle to the neighboring particles is determined. Afterwards, forces arising due to contacts are calculated by contact constitutive relation. The calculated forces in turn constitute input to calculate the motion for the next calculation step. This iterative calculation scheme is referred to as "calculation circle" (Figure 2.1). If the time is considered to be the third dimension of this calculation scheme, it can be conceived as a spiral rather than a circle.

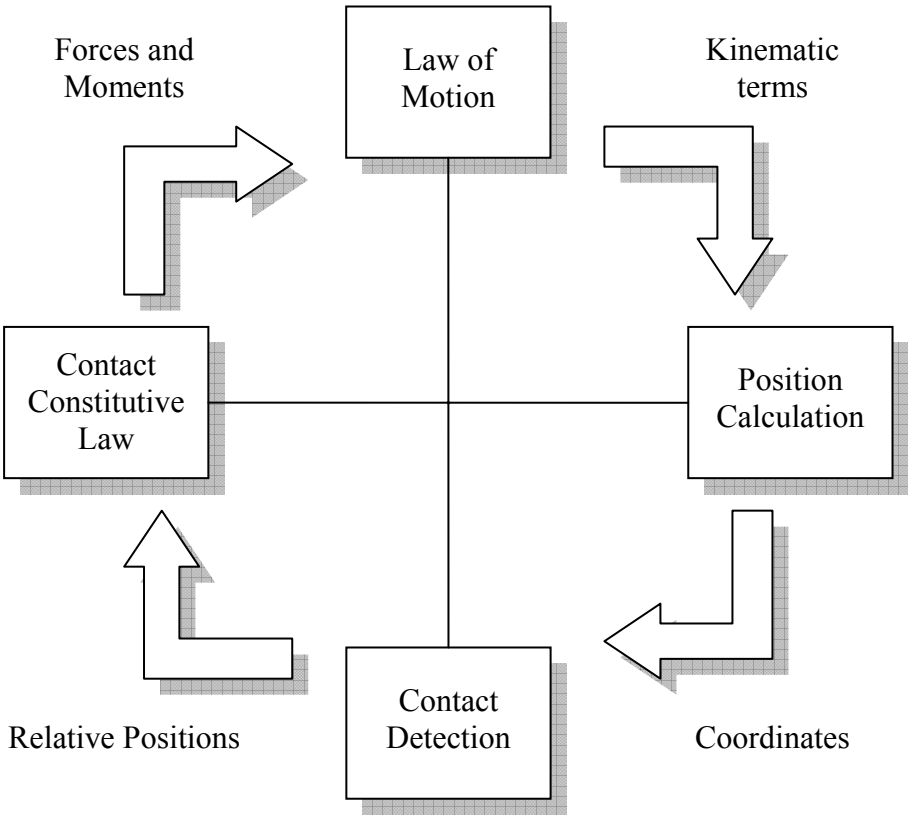


Figure 2.1 Calculation circle of Discrete Element Method

The theoretical formulations of the elements of this calculation scheme are articulated in following sections.

2.1.3 Velocity Issue

The nature of DEM is fully dynamic. Therefore, the term velocity is introduced. On the other hand, the geomechanical problems, even when truly dynamic, are generally idealized as static or quasi-static. Therefore, the effect of velocity (or rate of loading) inherent in DEM provides a new alternative concept for solution of geotechnical problems.

The effect of velocity with an analogy and the difference between the results of quasi-static and dynamic simulations is described in ABAQUS documentation very clearly. Figure 2.2 shows two cases of an elevator full of passengers. In the slow case the door opens and you walk in. To make room, the occupants adjacent to the door slowly push their neighbors, who in turn push their neighbors, and so on. This disturbance passes through the elevator until the people next to the walls indicate that they cannot move. A series of waves pass through the elevator until everyone has reached a new final equilibrium position. If you increase your speed slightly, you will shove your neighbors more forcefully than before, but in the end everyone will end up in the same position as in the slow case. In the fast case you run into the elevator at high speed, permitting the occupants no time to rearrange themselves to accommodate you. Two people directly in front of the door will be injured, while the other occupants will be unaffected.

Such effects, which exist for dynamic problems, can not be taken into consideration through quasi-static analyses. In the discrete element simulation of geomechanical problems, the rate of loading, which can affect the failure mechanism, is considered intrinsically. D'Addetta (2004) illustrated this effect of velocity to the failure mechanism through simulation of a retaining wall problem (Figure 2.3).

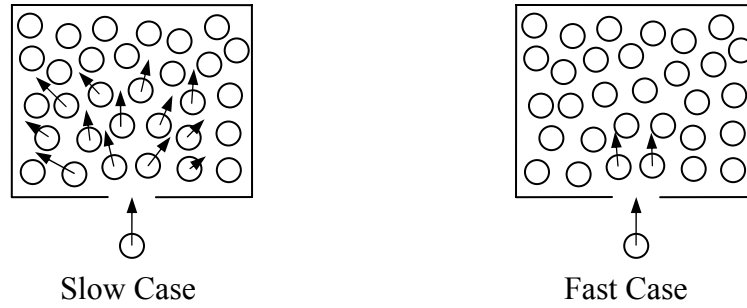


Figure 2.2 Illustration of the effect of velocity (rate of loading) (ABAQUS Documentation, 2004)

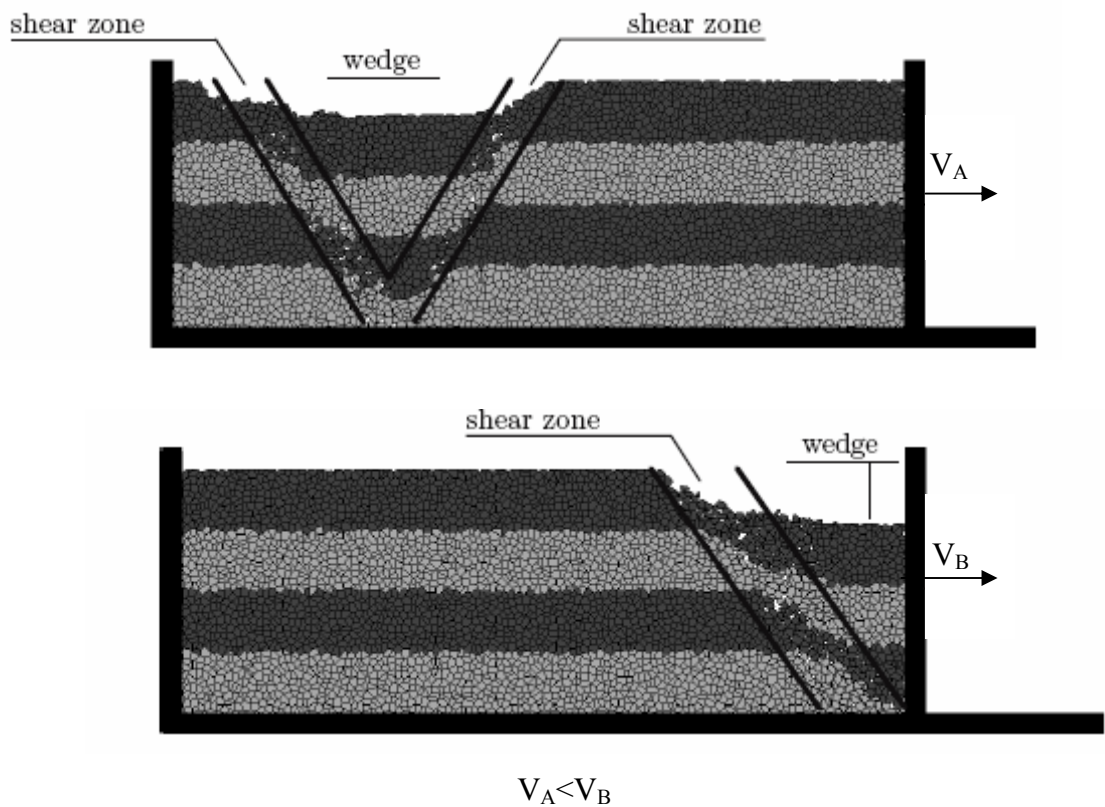


Figure 2.3 Effect of velocity to the failure mechanism of the backfill behind a retaining structure (D'Addetta, 2004)

2.1.4 Issues of Stress and Strain

In continuum based methods, the constitutive relation is defined as the relation between stress and strain. Nevertheless, the equivalent of this relation is between relative displacements and contact forces in the DEM. Therefore, the stress and strain are the valid terms for continuum rather than granular assemblies.

In the DEM, the micromechanical stresses and strains may be obtained through “Homogenization” techniques (Alonso-Marroquin, 2004). As Cambou, et al (1995) stated, homogenization is a general term of deriving macro-mechanical parameters of a material from its micro-mechanical properties. There are several ways of averaging techniques of micro-mechanical stress in the granular media but there is no accepted way of calculating strain tensor, as yet. There exist some studies on this subject (e.g. O’Sullivan, et al, 2003) and it is still under discussion.

Alonso-Marroquin and Herrmann (2005) studied the derivation of micro-mechanical stress and strain. Additionally, Itasca (2006) embedded their stress and strain calculation in the computer program PFC^{2D}/PFC^{3D} and gave the formulations in the manuals (Itasca, 2006).

2.1.5 Parameter Selection

In any kinds of numerical analyses, the parameters that define the material behavior need to be known or estimated. These parameters are normally obtained by either direct measurement of required parameter (like Young’s modulus) or using correlation relations (e.g. cohesion from plasticity index) from field or laboratory tests in geomechanics. Those tests generally measure the macro-mechanical properties of the materials. Therefore, these parameters can be directly used in continuum based numerical analysis.

Conversely, DEM requires micro-mechanical parameters and direct measurement tests of them are not common. Therefore, homogenization techniques are required to obtain these parameters from conventional tests. Cambou et al (1995) and Emeriault et al (1996) studied on homogenization for granular materials and introduced some relations between micro and macro elastic parameters. Ng (2006)

performed several sensitivity analyses in order to investigate the effects micro-mechanical parameters to the complete model.

Currently, a calibration phase may be necessary before starting analyses (Cundall, 2001). In this phase, a laboratory or field test model can be simulated and micro-mechanical parameters are iterated until reaching the required macro-mechanical properties. Then, the numerical analysis can be performed by these parameters. Obviously, calibration studies are tough and time consuming studies, therefore, more detailed and sophisticated investigations on this subject are required.

2.2 Theory of Motion and Position Calculation

The motion of a rigid body is defined by the motion of the center of mass assuming that any forces and moments act on that point. This point has three degrees of freedom (two transitional and one rotational) in two dimensions and six degrees of freedom (three translational and three rotational) in three dimensions.

The Newton's second law of motion is used to define the translational motion of the body as given in the equation below:

$$\bar{F} = m \cdot (\ddot{\bar{s}} - \bar{g}) \quad (2.1)$$

where,

\bar{F} : vector sum of the all applied forces,

m: total mass of the body,

$\ddot{\bar{s}}$: acceleration vector,

\bar{g} : body force acceleration vector (like gravity)

If the local coordinate system is assumed to lie along the principal axes of inertia, the equations of rotational motion in three dimensions are given by Euler (Hibbeler, 1989):

$$M_x = I_x \cdot \ddot{\phi}_x + (I_z - I_y) \cdot \ddot{\phi}_z \cdot \dot{\phi}_y \quad (2.2a)$$

$$M_y = I_y \cdot \ddot{\phi}_y + (I_x - I_z) \cdot \ddot{\phi}_x \cdot \dot{\phi}_z \quad (2.2b)$$

$$M_z = I_z \cdot \ddot{\phi}_z + (I_y - I_x) \cdot \ddot{\phi}_y \cdot \dot{\phi}_x \quad (2.2c)$$

where,

M_x, M_y, M_z : components of the moment,

I_x, I_y, I_z : principal mass moment of inertias,

$\ddot{\phi}_x, \ddot{\phi}_y, \ddot{\phi}_z$: components of angular acceleration,

In case the sphere or the disk with the mass distributed uniformly over the volume, the center of mass coincides with the particle center. All principal moments of inertia of spherical and disk-shaped particles are essentially equal at their center of mass which coincides with the center of geometry. Therefore, above equations reduce to the following vector equation for spherical and disk-shaped particles of radius R and mass m:

$$\vec{M} = I \cdot \vec{\ddot{\phi}} \quad (2.3)$$

where,

$$I = \frac{1}{2} mR^2 \text{ for disk (two dimensional)} \quad (2.4a)$$

$$I = \frac{2}{5} mR^2 \text{ for sphere (three dimensional)} \quad (2.4b)$$

If the time step (Δt) is small enough so that the accelerations are assumed to be constant within that time step, the above differential equations can be solved to find the particle motions (Itasca, 2006). For this purpose, the following equations can be used if the velocity terms are computed at the mid of the time step (i.e. $\Delta t/2$):

$$\vec{\ddot{s}}_t = \frac{1}{\Delta t} (\vec{\dot{s}}_{t+\Delta t/2} - \vec{\dot{s}}_{t-\Delta t/2}) \quad (2.5)$$

$$\vec{\ddot{\phi}}_t = \frac{1}{\Delta t} (\vec{\dot{\phi}}_{t+\Delta t/2} - \vec{\dot{\phi}}_{t-\Delta t/2}) \quad (2.6)$$

After implementing the equations of motions to the above formulae, the velocities for the next time step can be calculates as:

$$\vec{\dot{s}}_{t+\Delta/2} = \vec{\dot{s}}_{t-\Delta/2} + \left(\frac{\vec{F}_t}{m} + \vec{g} \right) \cdot \Delta t \quad (2.7)$$

$$\vec{\phi}_{t+\Delta/2} = \vec{\phi}_{t-\Delta/2} + \left(\frac{\vec{M}_t}{I} \right) \cdot \Delta t \quad (2.8)$$

Finally, the new position of the center of particle is:

$$\vec{s}_{t+\Delta t} = \vec{s}_t + \vec{s}_{t+\Delta t/2} \cdot \Delta t \quad (2.9)$$

The rotation of the particle can also be calculated but it does not have any significance in case of sphere or disk.

This solution technique is known as explicit finite difference procedure. In this procedure, the major concern is to decide the maximum stable time step in which the kinematical terms are assumed to be constant. This issue is discussed in Section 2.4 in detail.

2.3 Contact Constitutive Relations

In the DEM, the attitude of the particles that is in contact with the other particles or boundary elements is defined by the contact constitutive models. Contact constitutive model is a relation by which the forces arising due to the contact can be calculated from the relative positions of interacting particles. There exist various contact constitutive models. However, only the most widely used models for spherical and disk-shaped particles are discussed in this section.

The contact constitutive relations can be divided into three mutually exclusive models:

- Contact – stiffness models
- Contact – yield models
- Damping models

The first two models are the equivalents of elastic and plastic parts of any continuum based constitutive relations, respectively. That is to say, contact-stiffness models define the linear or nonlinear recoverable portion of contact relation,

whereas, contact–yield models characterize the failure of interaction between particles (either shear or tension failure).

Contact stiffness model is a compulsory contact constitution relation while the others are optional. However, it is recommended that at least the frictional linear contact model (refer to the following sections) which is the simplest and basic constitutive relation should be introduced as a contact–yield model to obtain healthy results.

Damping models are important and necessary for dissipating energy and damping of the oscillating motions, which are the natural outcome of the dynamic solution techniques.

2.3.1 Contact – Stiffness Models

Linear Contact Model

It is the most widely used contact constitutive model. The relation between the contact overlap distances and the developing forces are assumed to be linear in this model and simulated by linear springs in both normal and tangential directions.

Accordingly, the model can be formulated in scalar form as:

$$F_n = K_n \cdot \delta_n \quad (2.10a)$$

$$F_t = K_t \cdot \delta_t \quad (2.10b)$$

where,

F_n, F_t : magnitude of normal and tangential forces at contact

K_n, K_t : normal and tangential contact stiffness

δ_n, δ_t : normal and tangential overlap distances at contact

The vector form can easily be obtained by multiplying the above scalar forces by unit direction vectors of the contact.

If the contact stiffness parameters are defined as the particle property instead of contact property itself, the equivalent contact stiffness parameters can be obtained by the serial spring formulations:

$$K_n = \frac{k_{n,1} \cdot k_{n,2}}{k_{n,1} + k_{n,2}} \quad (2.11a)$$

$$K_t = \frac{k_{t,1} \cdot k_{t,2}}{k_{t,1} + k_{t,2}} \quad (2.11b)$$

where,

$k_{n,i}, k_{t,i}$: normal and tangential contact stiffness of individual particle.

This model also introduces an important discrete material parameter (λ); the ratio of the tangential stiffness to the normal stiffness, which is referred to as contact stiffness ratio.

$$\lambda = \frac{K_t}{K_n} \quad (2.12)$$

Hertz-Mindlin Contact Model

This model is based on the spherical contact studies of Hertz in normal force calculation and Mindlin and Deresiewicz in tangential force calculation (cited by van Baars, 1996). The forces at the contact are proportional to contact area rather than the overlap distance, consequently, the relation is non-linear.

The Hertz-Mindlin model is formulized as follows:

$$F_n = \frac{4}{3} \cdot \bar{E}^* \cdot \sqrt{R} \cdot \delta_n^{3/2} \quad (2.13)$$

$$F_t = 8 \cdot \bar{G}^* \cdot \sqrt{R \cdot \delta_n} \cdot \delta_t \quad (2.14)$$

where,

F_n, F_t : magnitude of normal and tangential forces at contact

δ_n, δ_t : normal and tangential overlap distances at contact

$$\bar{E}^* = \frac{E_1^* \cdot E_2^*}{E_1^* + E_2^*} \quad (2.15)$$

$$\bar{G}^* = \frac{G_1^* \cdot G_2^*}{G_1^* + G_2^*} \quad (2.16)$$

$$\bar{R} = \frac{R_1 \cdot R_2}{R_1 + R_2} \quad (2.17)$$

$$E^* = \frac{E}{1-\nu^2} = \frac{2 \cdot G}{1-\nu} \quad (2.18)$$

$$G^* = \frac{E}{2(1+\nu)(2-\nu)} = \frac{G}{2-\nu} \quad (2.19)$$

R: radius of particle

E: young modulus of particle

G: shear modulus of particle

ν : Poisson's ratio of particle

Note that;

$$G = \frac{E}{2 \cdot (1 + \nu)} \quad (2.20)$$

The similarity of this model with the linear contact model can be established as:

$$K_n = \frac{F_n}{\delta_n} = \frac{4}{3} \cdot \bar{E}^* \cdot \sqrt{\bar{R} \cdot \delta_n}$$

$$K_t = \frac{F_t}{\delta_t} = 8 \cdot \bar{G}^* \cdot \sqrt{\bar{R} \cdot \delta_n}$$

Accordingly, the contact stiffness ratio is:

$$\lambda = \frac{K_t}{K_n} = 6 \cdot \frac{\bar{G}^*}{\bar{E}^*} \quad (2.21)$$

If the elastic parameters of the two interacting spheres are equal, then:

$$\lambda = 3 \cdot \frac{1 - \nu}{2 - \nu} \quad (2.22)$$

This relation is quite useful since it apparently shows that the contact stiffness ratio is only a function of Poisson's ratio providing that the elastic properties of the contacting spheres are identical. This relation can also be used in linear contact model as well. It can be observed that:

$$K_t = K_n \rightarrow \lambda = 1 \text{ if } \nu = 0.5 \text{ and}$$

$$\text{For } \nu < 0.5 \rightarrow \lambda > 1 \rightarrow K_t > K_n$$

2.3.2 Contact – Yield Model

Slip Model

This model defines the friction between the particles and normally the default yield relation unless there is bond between particles. If the tangential (shear) force exceeds the frictional resistance of the contact, slipping occurs. The limiting tangential force is formulated as

$$F_{t,\max} = \mu \cdot F_n \quad (2.23)$$

where,

$F_{t,\max}$: limiting tangential force

F_n : magnitude of normal force at contact

μ : Coulomb's friction coefficient

When the tangential force is limited by the above value, the tangential overlapping distances should be back-calculated and updated in the relevant contact-stiffness computation.

Parallel Bond Model

In this model, there is a finite-sized glue bond between particles. After the bond is activated, the following forces in addition to the forces stemming from the contact-stiffness model develop:

$$\Delta F_n = -K_n \cdot A \cdot v_n \cdot \Delta t \quad (2.24)$$

$$\Delta F_t = -K_t \cdot A \cdot v_t \cdot \Delta t \quad (2.25)$$

$$\Delta M_n = -K_n \cdot J \cdot \omega_n \cdot \Delta t \quad (2.26)$$

$$\Delta M_t = -K_t \cdot \frac{J}{2} \cdot \omega_t \cdot \Delta t \quad (2.27)$$

where,

$$A = \pi \cdot \bar{R}^2 : \text{area of the bond}$$

$$J = \frac{1}{2} \pi \cdot \bar{R}^4 : \text{polar moment of inertia of the particle cross section.}$$

The bond is broken if the tensile or shear stresses exceed the predefined values. The permissible bond stresses are formulated as:

$$\sigma_{\max} = \frac{F_n}{A} + \frac{2 \cdot M_t}{J} \cdot \bar{R} \quad (2.28)$$

$$\tau_{\max} = \frac{F_t}{A} + \frac{M_n}{J} \cdot \bar{R} \quad (2.29)$$

The derivation and detailed studies on bonded particle model represented above are given by Potyondya and Cundall (2004).

2.3.3 Damping models

Although the energy in the system can be dissipated by the friction between the particles, additional damping force may be required in order to damp the redundant oscillations and to reach equilibrium conditions more quickly. The damping models provide additional forces in the opposite direction to that of the motion to dissipate the velocity. There exist several damping methods. They can be investigated under two separate groups:

- Viscous damping
- Non-viscous damping

Viscous damping force is the function of velocity. It is widely used in dynamic structural analyses to dissipate energy. On the other hand, the damping force is a proportion of the existing force in non-viscous damping, which acts opposite direction to the motion. That is to say, non-viscous damping force damps acceleration (consequently the unbalanced force that causes motion) rather than velocity. Therefore non-viscous damping is more effective in quasi-static system since it will help the system reach equilibrium more quickly. The most common non-viscous damping is the due to the friction between the bodies. Some of widely used damping models are investigated below:

Viscous Damping Model

In viscous damping, normal and shear dashpots are provided in addition to the springs that represent the contact stiffness as illustrated in Figure 2.4

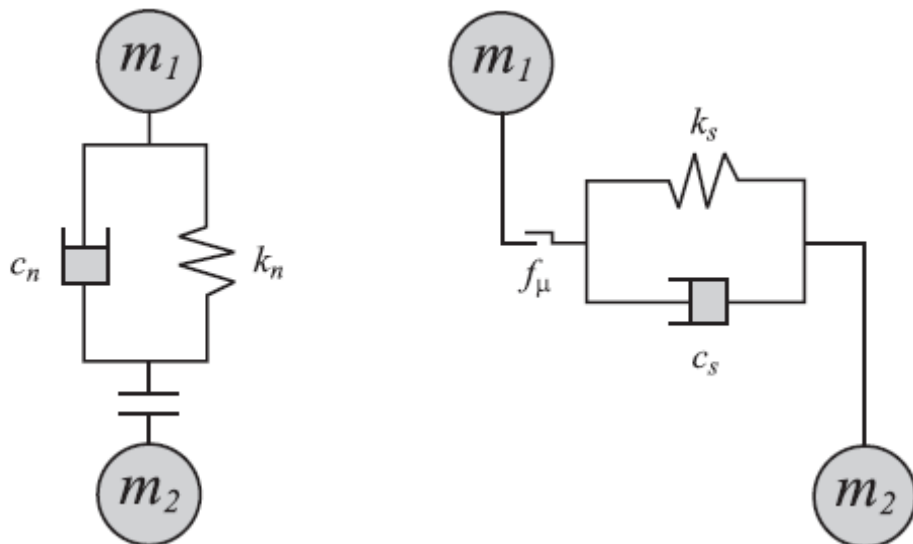


Figure 2.4 Illustration of viscous damping between particles (Itasca, 2006)

Damping forces components are;

$$D_n = c_n \cdot |v_n| \quad (2.30a)$$

$$D_t = c_t \cdot |v_t| \quad (2.30b)$$

where,

D_n, D_t : normal and tangential damping forces

c_n, c_t : normal and tangential damping constants

v_n, v_t : normal and tangential relative velocities at the contact

Damping constants c_n, c_t can be given directly or expressed in a fraction of critical damping constants as:

$$c_n = \beta_n c_n^{\text{crit}} \quad (2.31a)$$

$$c_t = \beta_t c_t^{\text{crit}} \quad (2.31b)$$

Critical damping constants are,

$$c_n^{\text{crit}} = 2\sqrt{\bar{m} \cdot K_n} \quad (2.32a)$$

$$c_t^{\text{crit}} = 2\sqrt{\bar{m} \cdot K_t} \quad (2.32b)$$

where,

$$\bar{m} = \frac{m_1 \cdot m_2}{m_1 + m_2} \quad (2.33)$$

Non-viscous Damping Models

Frictional damping:

If the slip model (Section 2.3.2) is introduced to the system, the energy at the contact will be dissipated due to the existence of friction.

Local damping:

Another damping method is the so called local damping (Itasca, 2006). In this method, damping force term is added to the equation of motion as:

$$\bar{\mathbf{F}} + \bar{\mathbf{F}}_d = m \cdot \bar{\mathbf{s}} \quad (2.34)$$

$$\bar{\mathbf{M}} + \bar{\mathbf{M}}_d = I \cdot \bar{\boldsymbol{\phi}} \quad (2.35)$$

where,

$\bar{\mathbf{F}}_d, \bar{\mathbf{M}}_d$: damping force and moment vectors, respectively.

It is assumed that the damping forces and moments are directly proportional to the forces and moments acting on a body but in the opposite direction to the motion. The components of the damping forces and moments are expressed as follows.

$$F_{x,d} = -\alpha \times \text{sign}(v_x) \times |F_x| \quad (2.36a)$$

$$F_{y,d} = -\alpha \times \text{sign}(v_y) \times |F_y| \quad (2.36b)$$

$$F_{z,d} = -\alpha \times \text{sign}(v_z) \times |F_z| \quad (2.36c)$$

$$M_{x,d} = -\alpha \times \text{sign}(\omega_x) \times |M_x| \quad (2.36d)$$

$$M_{y,d} = -\alpha \times \text{sign}(\omega_y) \times |M_y| \quad (2.36e)$$

$$M_{z,d} = -\alpha \times \text{sign}(\omega_z) \times |M_z| \quad (2.36f)$$

where,

α : non-dimensional damping constant

v_x, v_y, v_z : components of translational velocity of particle

$\omega_x, \omega_y, \omega_z$: components of rotational velocity of particle

The default value of damping constant is proposed as 0.7 in PFC^{2D}/PFC^{3D}.

Damping from restitution

When two particles collide, a part of the kinetic energy before the impact is dissipated or dispersed. There is a term to represent this energy dissipation so called coefficient of restitution (e) which is defined as the ratio of restitution impulse to the deformation impulse (Hibbeler, 1989). It is formulated as

$$e = \frac{v_r}{v_i} \quad (2.37)$$

where,

e : coefficient of restitution

v_r, v_i : rebound and incident impact velocities, respectively.

The force necessary to maintain this phenomenon is expressed as follows (DEM Solutions, 2006):

$$F_d = -2 \cdot \beta \cdot v \cdot \delta^{1/4} \sqrt{\frac{10}{3} \bar{m} \cdot \bar{E} \cdot \bar{R}^{1/2}} \quad (2.38)$$

where,

$$\beta = \frac{\ln(e)}{\sqrt{\pi^2 + [\ln(e)]^2}}$$

v : relative velocity

δ : overlapping distance

$$\bar{E} = \frac{E_1 \cdot E_2}{E_1 + E_2} \quad (2.39)$$

\bar{m} and \bar{R} are defined in equations 2.33 and 2.17 respectively.

This type of damping is effective in relatively high speed and completely discrete situations but not enough for damping of closely packed assemblies.

2.4 Stable Time Step

As discussed earlier, computation time is the major shortcoming of the DEM. Therefore, time step which is used in the finite different integration of motion given in Section 2.2 should be maximized while maintaining the solution stability.

Theoretically, the maximum stable time step is related to the minimum Eigen period of the total system. However, it is not practical to perform Eigen value analysis in DEM simulations. Therefore, some approximations are necessary to determine critical time. For a single degree of freedom (SDOF) system critical time step is expressed as (cited by Itasca, 2006):

$$t_{\text{critical}} = \frac{T}{\pi} \quad (2.40)$$

where,

$T = 2\pi\sqrt{m/k}$, period of SDOF system

m: mass

k: spring stiffness

Rayleigh time step is an important feature for DEM simulations. This is the time taken for a shear wave to propagate through a solid particle. It is therefore a theoretical maximum time step for a DEM simulation of a quasi-static particulate collection in which the coordination number (total number of contacts per particle) for each particle remains above one (DEM Solutions, 2006). It is given by,

$$t_{\text{critical}} = \frac{\pi \cdot R \cdot \sqrt{\rho / G}}{0.1631 \cdot \nu + 0.8766} \quad (2.41)$$

where,

R: radius of particle,

ρ : density

G: shear modulus

ν : Poisson's ratio

Within the stable time, maximum possible overlap distance must also be maintained. Therefore, for highly dynamic cases, Hertzian contact time can be important. Total contact time from Hertz theory of elastic collision is expressed as:

$$t_{\text{critical}} = 2.9432 \cdot \sqrt[5]{\frac{25}{64} \cdot \frac{\gamma}{\Delta v}} \text{ m}^2 \quad (2.42)$$

where,

$$\gamma = \frac{9}{16} \frac{1}{R} \left(\frac{1 - \nu}{G} \right)^2$$

m: mass

Δv : relative velocity at contact

R: radius

G: shear modulus

ν : Poisson's ratio

Obviously, critical time step is the theoretically maximum allowable time step. Therefore, the stable time should be a fraction of critical time step. As a general approach 10% to 20% of critical time step can be considered as appropriate.

It is noticeable that, stable time step is directly proportional to the mass (see equations 2.40, 2.41, 2.42). However, for static systems, mass is not an important parameter (except the body forces). Therefore, for static systems, density and consequently the mass of particle can be scaled up in order to increase the time step and reduce calculation time. However, in that case the time is not a real time and it may be more appropriate to call it calculation step.

2.5 Other Forms of DEM

As stated earlier, the focus in this study is on spherical particles. However, the shape of granular materials like sand is not spherical in reality. Calvetti, et al (2003) showed in their studies that friction angles of packing spheres are lower than the experimental values (cited by Alonso-Marroquin, 2004). Obviously, it is due to the fact that the rotational resistance of spherical particles is less than that of any arbitrarily shaped grains.

There are several studies on the DEM with different shaped grains. For instance, Cundall (1988) and Hart, et al (1988) presented their studies on three dimensional DEM with polyhedral blocks. However, the calculation time is the major shortcoming for arbitrarily shaped particles, as yet.

Ng (1992) proposed to use elliptical particles in DEM since the contact detection of ellipse is relatively simpler than any arbitrary shaped particles. Besides, the rotational resistance of elliptical particles is greater than that of spheres.

It may be possible to create arbitrary shaped particles by using the cluster of spherical particles (Favier et al, 1999). In this approach, spherical particles with varying or constant diameters are rigidly connected in order to form any random shape. Accordingly, the effort for contact detection remains unchanged while the equation of motion can be applied to the multi-element cluster. The example particles formed by this approach are shown in Figure 2.5.

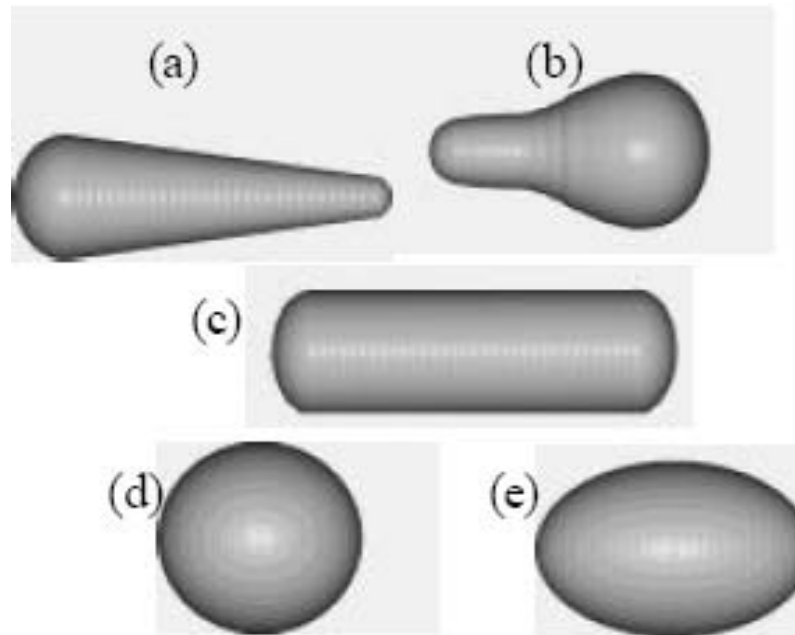


Figure 2.5 Example of multi-element clusters (Favier, 1999)

Sallam (2004) also studied on the modeling of angular soil particles by combining round elements in his PhD thesis. There is a special two-dimensional DEM program with concave polygonal shaped particles which is developed in University of Stuttgart and some studies are performed by this program (Alonso-Marroquin, 2004, D'Addetta, 2004, D'Addetta and Ramm, 2005). Linear shaped particles in two-dimension (Anandarajah, 1994) and plate shaped particles in three-dimension (Yao and Anandarajah, 2003) were proposed as well in order to simulate the clayey soil behavior.

O'Sullivan et al (2002) investigated the influence of particle angularity on the behavior of granular materials. As the conclusion of their studies, they stated that:

- Assemblies of angular particles are more compressible than that of rounded particles.

- Higher densities can be achieved with increasing particle angularity under the same magnitude of confining pressure.
- The peak shear strength for angular material occurs at a higher axial strain than for rounded particles, and there is a less significant reduction in post-peak strength.
- Shear strength is directly proportional to the number of angularity in particles.

In addition to particle shape, there are other different approaches to DEM. Van Baars (1996) introduced an implicit time integration scheme for essentially static systems. Bardet and Proubet (1991) proposed another solution scheme named adaptive dynamic relaxation to reduce the calculation time. There are also studies on coupled or hybrid DEM-FEM formulations (Munjiza, 2004). Shamy and Zeghal (2005) represented a study on coupled DEM-FEM analysis to model pore water in discrete assemblies.

CHAPTER 3

APPLICATION OF DEM ON BEARING CAPACITY PROBLEMS

3.1 Introducing the DEM Software EDEM™

3.1.1 General

A general-purpose DEM software, EDEM™ is used in the entire DEM analyses and simulations performed within the scope of this study. EDEM™ is commercial DEM software for simulation of three-dimensional particle mechanics. It is developed and distributed by DEM Solutions Ltd.

EDEM™ has a very user friendly and easy-to-use graphical user interface (GUI) as illustrated in. Figure 3.1. It is the most professional DEM software available in the market currently. On the other hand, since it is not particularly designed for geotechnical applications, creation and working with closely packed assemblies in static or nearly static condition can sometimes be problematic.

The capabilities and theoretical background of the software are discussed briefly in the following sections.

3.1.2 Element types

Program consists of two types of elements:

- Particle elements
- Geometry elements.

Particle elements are rigid elements with deformable contact surface. The particles can be a single sphere or cluster of several spheres (Favier, 1999). Particles are produced and introduced into the model by an efficient engine named “Particle Factory™”. It is also possible to create user-defined particle arrangements.

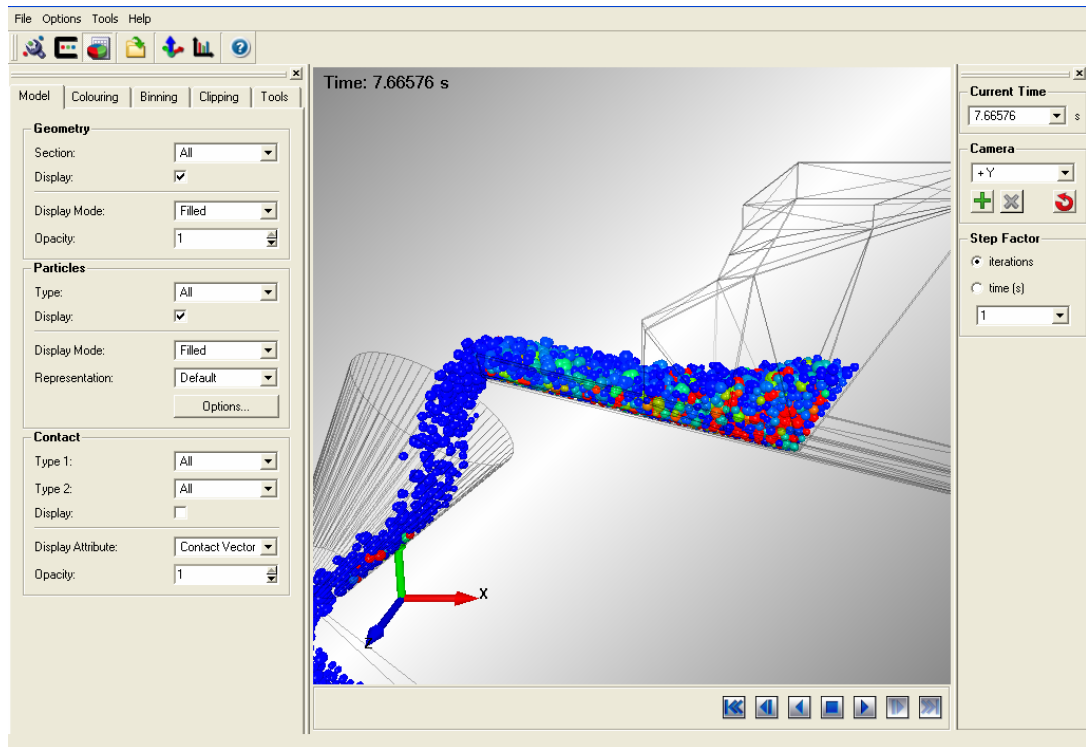


Figure 3.1 Illustration of EDEM™ user interface

Geometry elements are for creation of boundary conditions to the particulate media. They are not deformable and their motion is controlled by the user by specifying prescribed velocity or acceleration. The geometry elements can be either created inside the program or imported from any Computer Aided Drawing (CAD) programs. EDEM™ uses triangulation technique to define the surface of any geometry elements.

3.1.3 Computation technique

EDEM™ is completely dynamic in real time domain. The Newton's second law of motion is used to define the activity of the particles as described in Section 2.2. Therefore, it exploits explicit finite difference solution technique.

The program has parallel processing capability for dual-processor computers.

It is possible to introduce body force acceleration (like gravity) to the particles. Besides, the program accepts any user-defined external forces. However, those forces can only be applied to the particles.

3.1.4 Contact models

The only internal contact constitutive relation offered by EDEM™ is Hertz – Mindlin model (see Section 2.3.1). However, four additional user-defined models are provided with the program both in source and binary forms. Those are listed and briefly explained below:

- Linear Spring Contact Model: Its theory is given in 2.3.1. There is no damping in this model. However the tangential force is subject to the limit imposed by friction.
- Parallel Bond Contact Model: This model is provided to bond the particles by a finite-sized “glue” bond. This bond can resist tangential and normal movements up to a maximum normal and tangential shear stresses, at which point the bond breaks. Thereafter the particles interact as hard spheres. This model is particularly suited to model continuum like concrete and rock structures.
- Cohesion Contact Model: This model modifies Hertz-Mindlin contact by adding a normal cohesion force.
- Moving Plane Contact Model: This model simulates a linear motion of a geometry section. The whole section is deemed to move at the same velocity. The contact model adds this linear velocity to the velocity of the geometry section only within the contact model (so the geometry section does not actually move). This model is suitable for simulation of transportation of bulk materials such as conveyor belts.

It is possible to add user-defined contact constitutive relation to the program. For this purpose, the provided codes can be modified and compiled as dynamic linked library (dll) in Microsoft Windows – shared object (so) in Linux.

3.1.5 Post-Processor

EDEM™ has quite useful post-processor to investigate any computed results. It can animate the motion of the particles in timely fashion. It is possible to colorize the particles and/or the contacts regarding the any computed value such as velocity, contact force, etc. The result of any calculated value can be exported out to interpret in any other software. EDEM™ can also prepare charts and graphs for illumination of results.

3.2 Analysis Procedure

The predictive capacity of the DEM in any fields of application as well as bearing capacity problems can be investigated through comparison with the results of other numerical analysis techniques or analytical methods. However, application of DEM requires calibration studied as explained by Cundall (2001) since the parameters in either method should be comparable.

In order to obtain macro-mechanical parameters, two separate test platforms are prepared:

- Isotropic compression test platform to measure macro elastic parameters of the model
- Direct shear test platform to measure the strength parameters.

Due to the nature of the DEM, it is not possible to get the same geometry for different models that are randomly filled by particles. The arrangement of particles (especially for coarse filling) may affect the results of the analysis in spite that the micro-mechanical parameters are the same. For this reason, a user defined particle factory code is generated to map the particle arrangement and re-produce for different runs. Such mapping technique brings another advantage of reducing calculation time that is spent for model generation.

A computer having 2×2.0 GHz dual-processors with 2 GB of RAM is utilized for DEM simulations. The calculation times can be expressed in days for the simulations carried out in the scope of this study.

One of the major advantages of numerical analysis is to have the chance of analyzing exactly the same geometry several times and in several studies. In this study, the DEM model generated for bearing capacity analysis is also used in calibration studies in full scale.

The procedure for DEM analysis of bearing capacity problem is listed below:

- First of all the micro-mechanical parameters that is used in the analysis are to be defined. While selecting the model parameters, it is considered to reduce the calculation time and increase the visual quality (for better realization of the mechanisms) with minimum effect on solution reliability. Therefore, the material density is 10 times scaled up and the shear modulus of particles is selected lower than the real value to reduce the computation time. Since the model is relatively small when it is compared with the particle size, density scaling is helpful to increase the stresses values and exaggerate the displacements for better visualization. However, the solution time is not “real time” but it is a representative of calculation cycle. The selected micro-mechanical parameters are listed in Table 3.1.
- The model geometry is to be generated. For this reason, a box that is small in one dimension compared to the others to represent the plane strain condition is placed and filled with particles. Since EDEM™ does not allow the randomly generated particles to interact during filling process, the particle arrangement is extremely loose at this stage. Therefore, gravity is applied to compact the particles. This compaction process is to be continued until the energy within the system is dissipated and steady condition is reached. Unfortunately, damping method of EDEM™ is not effective for closely packed particles thus it is extremely time consuming to reach equilibrium. The physical properties of the geometric DEM model illustrated in Figure 3.2 are given in Table 3.2.
- The generated model is to be mapped for future geometry generation.
- Calibration runs is to be performed. The macro-mechanical parameters obtained from the calibration runs are the input parameters of both analytical and FEM solution of the problem.

- Analytical solutions are to be achieved by using the macro-mechanical yield parameters.
- The FEM analysis of the same model with the macro-mechanical parameters obtained from calibration runs is to be conducted. For this purpose, the plane strain FEM software Phase2 v6 is used.
- The bearing capacity analysis by DEM is to be accomplished and the results are to be compared.

The selected micro-mechanical parameters and properties of the geometric model are given in Table 3.1 and Table 3.2, respectively.

Table 3.1 Micro-mechanical parameters selected for analyses

Contact Constitutive Model	Hertz – Mindlin Non-linear contact formulation
Shear Modulus	1×10^8 Pa
Poisson's ratio	0.4
Density *	26 000 kg/m ³
Coefficient of Restitution	1×10^{-4}
Coefficient of Static Friction	0.5
Particle Diameter	48 ~72 mm (Average 60 mm)

* Density is 10 times scaled up.

Table 3.2 Properties of geometric model

Model Dimensions (X × Y × Z)	1500×120×700 mm
Total Volume	0.126 m ³
Total Weight of the Model *	16.95 kN
Unit Weight of Soil *	134.5 kN/m ³
Volume of Solids	0.0652 m ³
Void Ratio	0.52
Number of Particles	700

* Density is 10 times scaled up.

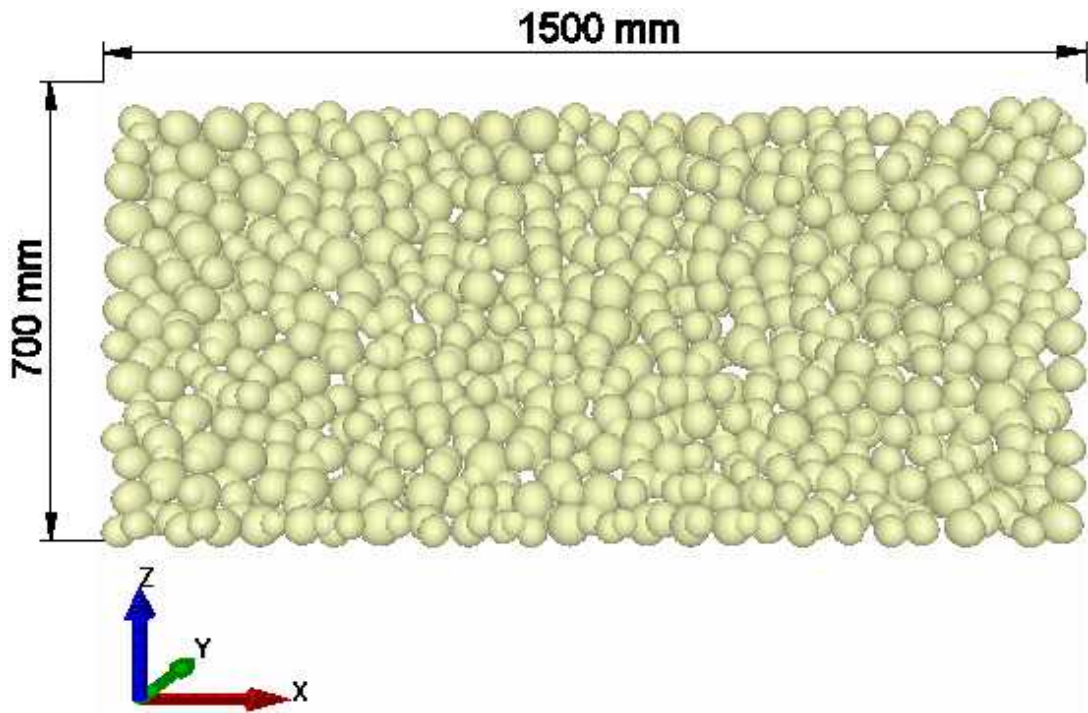


Figure 3.2 Generated input model

3.3 Calibration Runs

3.3.1 Isotropic Compression Test Simulation

The purpose of this simulation is to obtain macro-mechanical elastic parameters which are necessary for FEM simulation. As most of the FEM based softwares, Phase² requires Young's modulus (E) and Poisson's ration (ν) as the elastic properties of the material. These parameters can be obtained by making use of Hooke's law:

$$\varepsilon_x = \frac{1}{E} [\sigma_x - \nu(\sigma_y + \sigma_z)] \quad (3.1a)$$

$$\varepsilon_y = \frac{1}{E} [\sigma_y - \nu(\sigma_x + \sigma_z)] \quad (3.1b)$$

$$\varepsilon_z = \frac{1}{E} [\sigma_z - \nu(\sigma_x + \sigma_y)] \quad (3.1c)$$

During the isotropic compression test simulation, the X and Y directions are fixed while the material is compressed in Z direction. In this case,

$$\varepsilon_x = \varepsilon_y = 0$$

If the equations 3.1 are re-arranged, one can find that,

$$K = \frac{\sigma_x}{\sigma_z} = \frac{\nu}{1-\nu} \longrightarrow \nu = \frac{K}{1+K} \quad (3.2)$$

$$E = \frac{(1+\nu)(1-2\nu)}{1-\nu} \frac{\sigma_z}{\varepsilon_z} \quad (3.3)$$

The DEM simulation steps of the isotropic compression test are as follows:

- The previously generated model is placed into a box with the original dimensions of the model (1500×120×700 mm).
- The gravity in the system is removed.
- A plate is placed on top of the box and it is lowered in 5 steps to squeeze the particles inside the box.
- It is assured that the equilibrium is satisfied at the end of each step.
- Sum of the forces exerted by the particles to each wall is measured. Then the pressures are calculated.

Variation of the forces in X and Y directions during the calculation process are illustrated in Figure 3.5. The values extracted from measurements are given in Table 3.3.

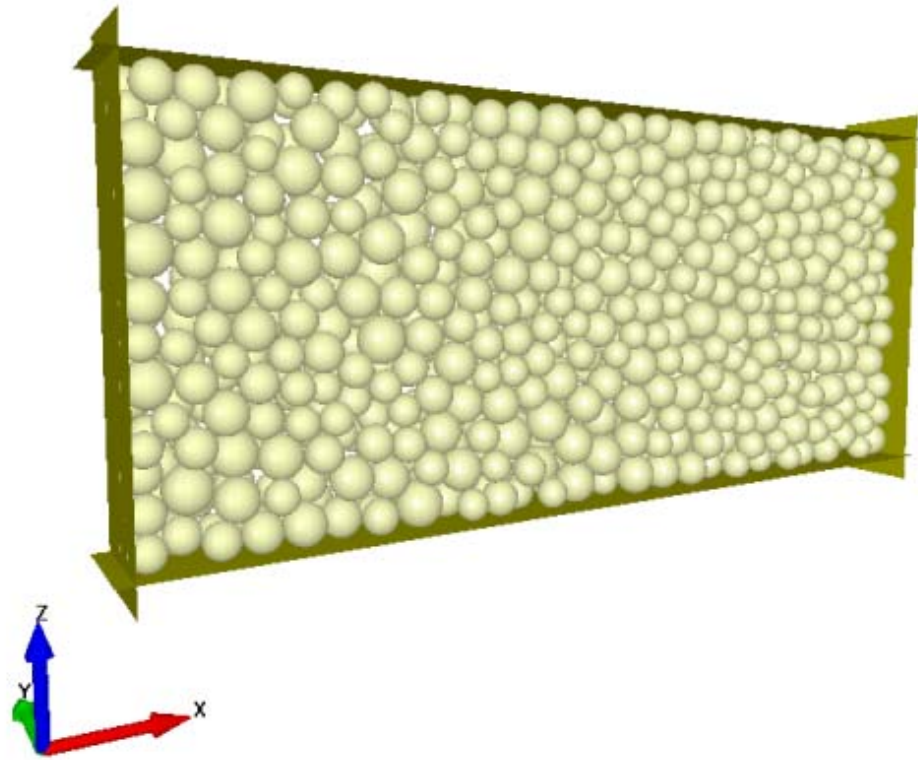


Figure 3.3 Isotropic compression test model

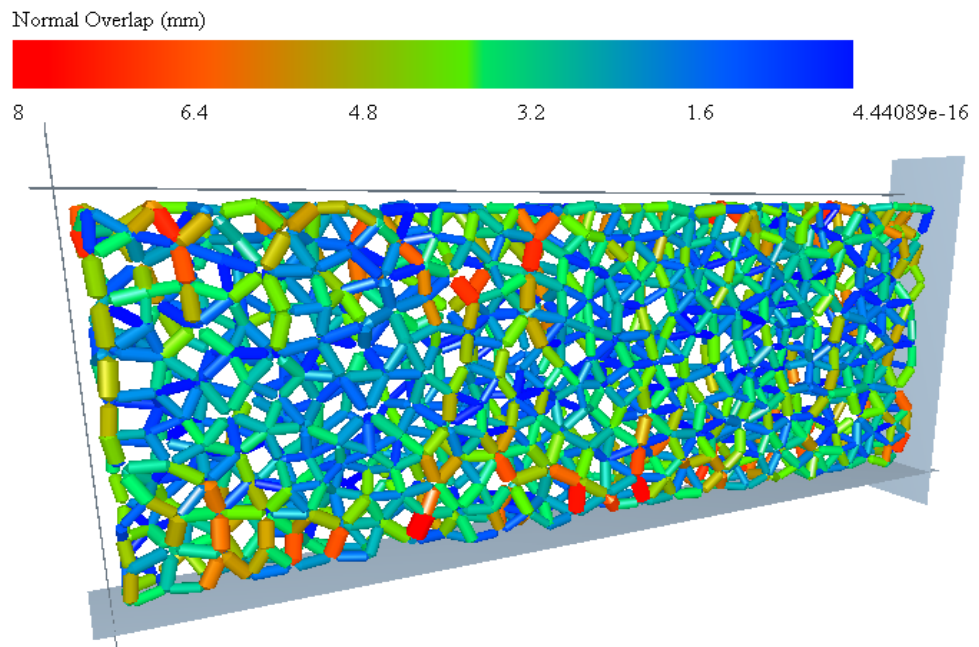


Figure 3.4 Contact overlap distance at the final stage of isotropic compression test

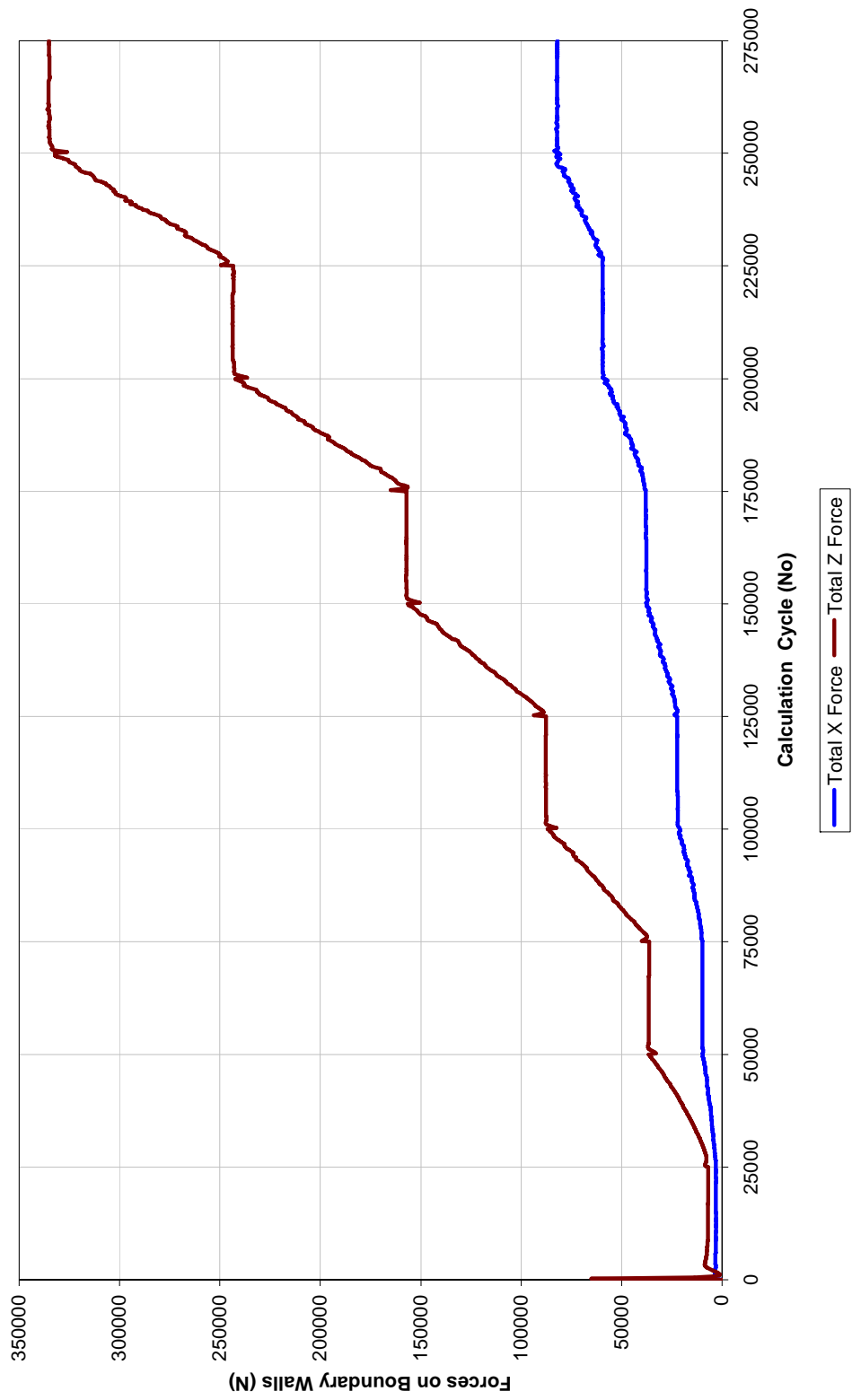


Figure 3.5 Measured forces during isotropic compression test simulation

Table 3.3 Results from isotropic compression test

Calculation Cycle at Equilibrium	Model Dimensions (mm)	Boundary Wall Forces (kN)		Stresses (kPa)		Axial Strain
		F_x	F_z	σ_x	σ_z	ϵ_z
25 000	1500 120 680	3.05	6,83	37.4	37.9	-
75 000	1500 120 660	9,80	36.32	123.7	201.8	0.0294
125 000	1500 120 640	22.36	87.61	291.1	486.7	0.0588
175 000	1500 120 620	37.95	157.12	510.1	872.9	0.0882
225 000	1500 120 600	59.40	243.35	825.0	1351.9	0.1176
275 000	1500 120 580	82.00	335.15	1178.2	1861.9	0.1471

If the first results obtained at the cycle of 25 000 is assumed as the starting point of the test, the tangential modulus of elasticity can be obtained from the differences of stress and strain as in Table 3.4. The strain versus stress diagram in principal directions is illustrated in Figure 3.6.

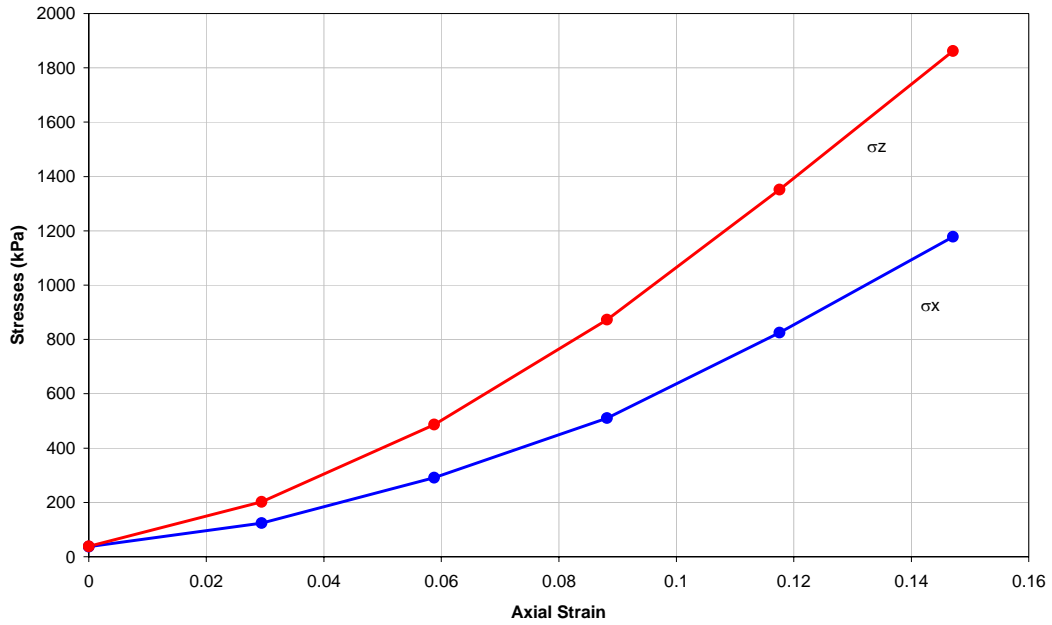


Figure 3.6 Variation of stresses in isotropic compression test

Table 3.4 Calculation of macro-elastic parameters

Stress Increments (kPa)		Axial Strain Increment	K	ν	E (kPa)
$\Delta\sigma_x$	$\Delta\sigma_z$	$\Delta\varepsilon_z$	σ_x / σ_z	Eq. 3.2	Eq. 3.3
86.3	163.9	0.0294	0.61	0.38	3667
167.4	284.9	0.0588	0.60	0.38	4422
219.0	386.2	0.0882	0.58	0.37	5596
314.9	479.0	0.1176	0.61	0.38	6141
353.2	510.0	0.1471	0.63	0.39	6345

Since the stress levels are closer to the later measurements and the variation is more stabilized, the macro-mechanical elastic properties of the material are selected as;

$$E = 6300 \text{ kPa}$$

$$\nu = 0.38$$

3.3.2 Direct Shear Test Simulation

Yield parameters are the other required macro-mechanical properties of the tested material. They are necessary for both FEM analysis and analytical solutions. Assuming the material obeys Mohr-Coulomb yield criterion, the direct shear test simulation is the most suitable testing method due to its simplicity and reliability (Masson and Martinez, 2001). The shear strength of the material in Mohr-Coulomb yield criterion is formulated as,

$$\tau = c + \sigma \cdot \tan \phi \quad (3.4)$$

where,

τ : shear strength of material

σ : normal stress

c: cohesion

ϕ : internal friction angle

Since there are no bonds between the particles in this model, the cohesion term vanishes. Therefore, the internal friction angle is,

$$\phi = \tan^{-1} \frac{\tau}{\sigma} \quad (3.5)$$

In real direct shear box tests, normally a constant load in normal direction is applied and the shear force is measured while the box is shearing. This process is repeated by changing the normal force. The slope of the normal force versus shear force diagram at failure gives the friction angle. However, it is not possible to apply prescribed forces to the geometry elements in EDEM™. For that reason, the constant volume direct shear method is employed as advised by Zhang and Thornton (2002). In this test, the volume is adjusted before starting the test and both shear and normal forces are measured during shearing process. The internal friction angle can be predicted by observing shear displacement (or strain) versus ratio of shear force to normal force diagram.

The steps followed during the DEM simulation of constant volume direct shear test is given below:

- The previously generated model is placed into two boxes located such that one is top of the other.
- Then a plate is placed onto the top box and it is lowered to compress the material. Iteration is continued until the steady state is reached (Figure 3.9).
- Shearing process is started. To ensure better force distribution, both boxes are displaced in opposite directions. During the test, the variation of the forces in X and Z directions are measured. Due to the existence of friction at the walls, the summation of all forces including the shear forces at the walls should be used in order to find the forces at the shear plane.

The variation of normal stress and the shear to normal force ratio on the shear plane are shown in Figure 3.7 and Figure 3.8, respectively.

It is realized that the normal stress in direct shear test tends to increase. This means that the material is trying to dilate during shear.

It is also observed that the variation of the friction is non-linear. The ultimate value of friction is around 0.75 that corresponds to internal friction angle (ϕ) of approximately 37° . However, it can be assumed that the yield is reached at T to N ratio of 0.65 ($\phi=33^\circ$).

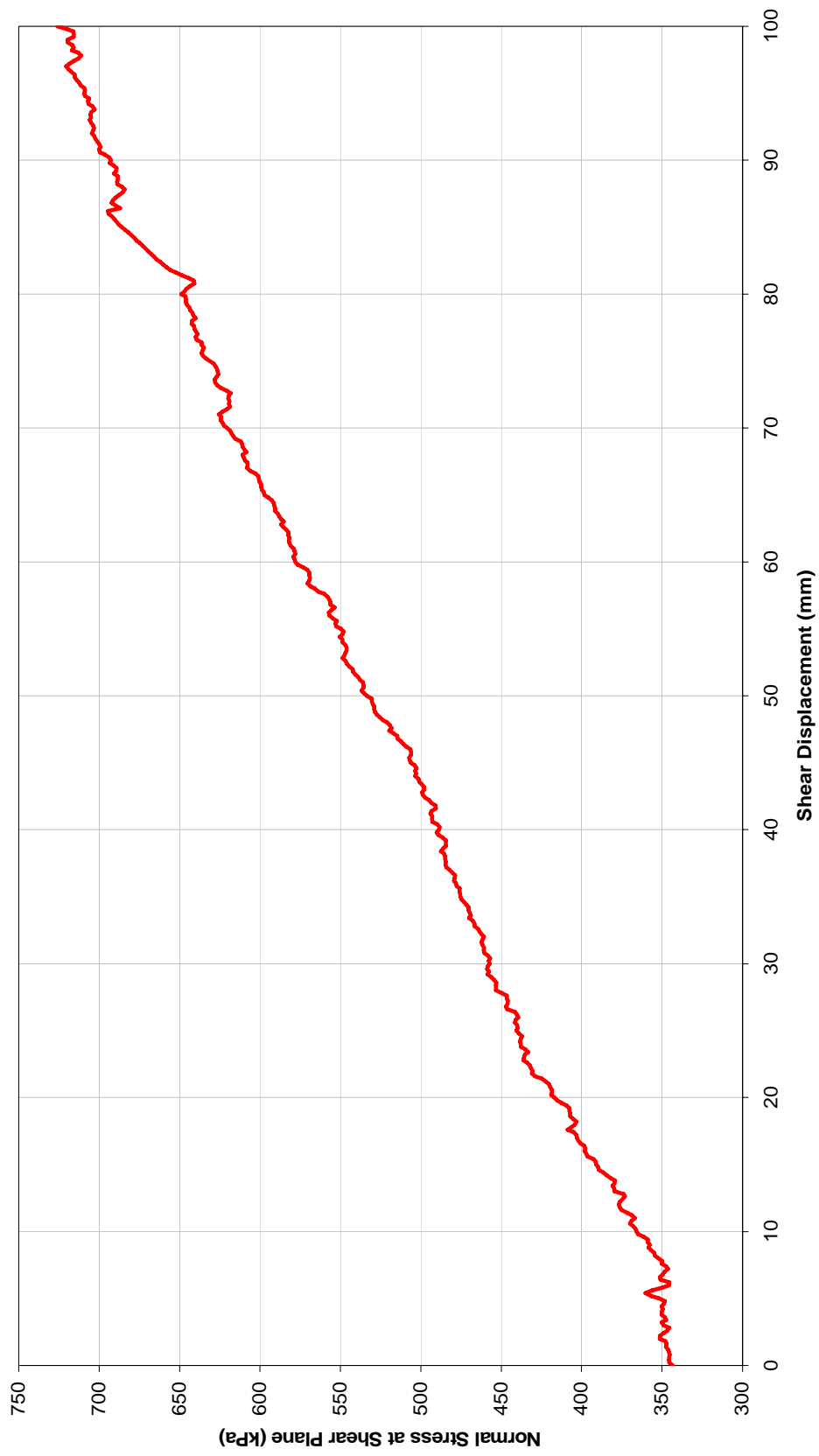


Figure 3.7 Variation of normal stress on shear plane

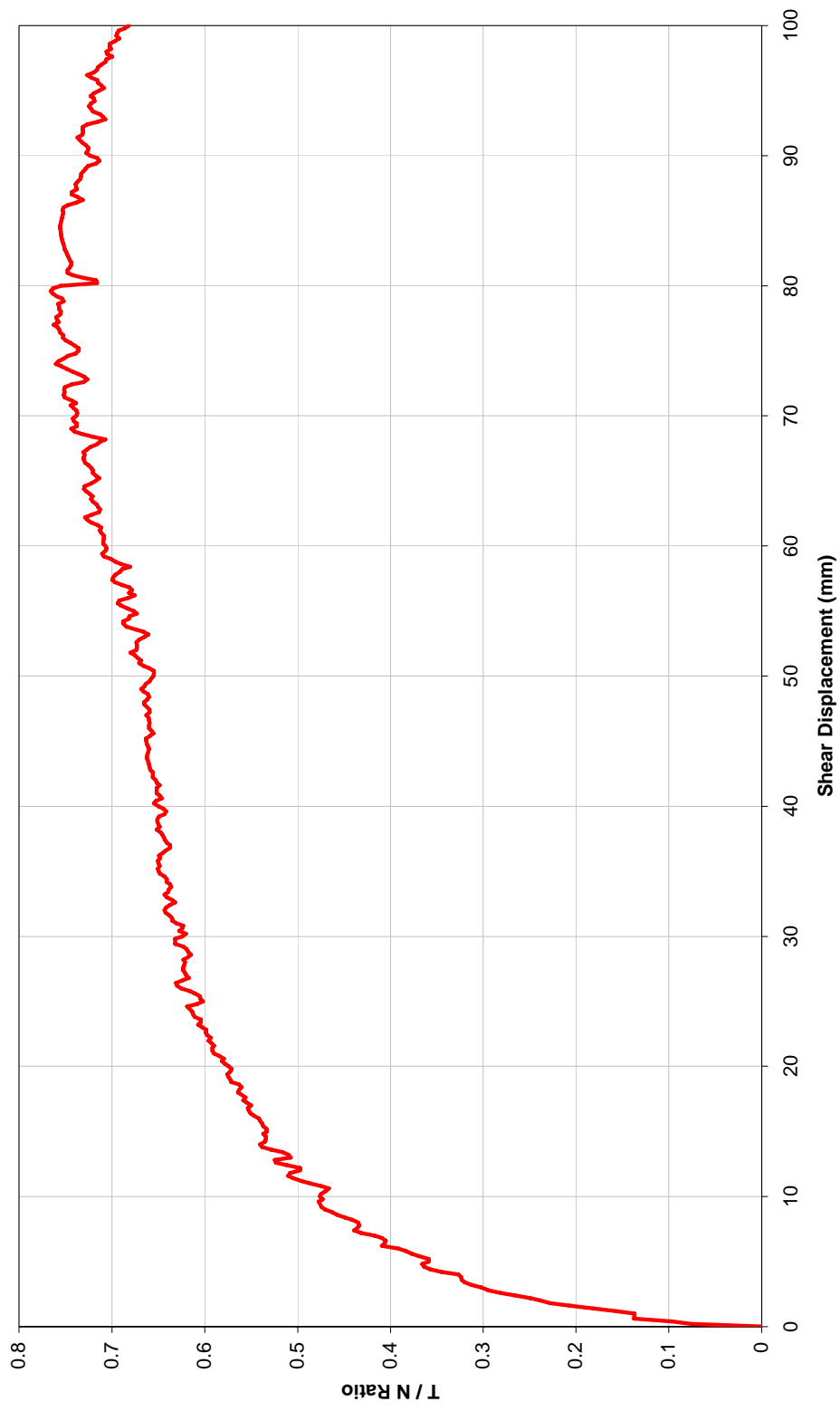
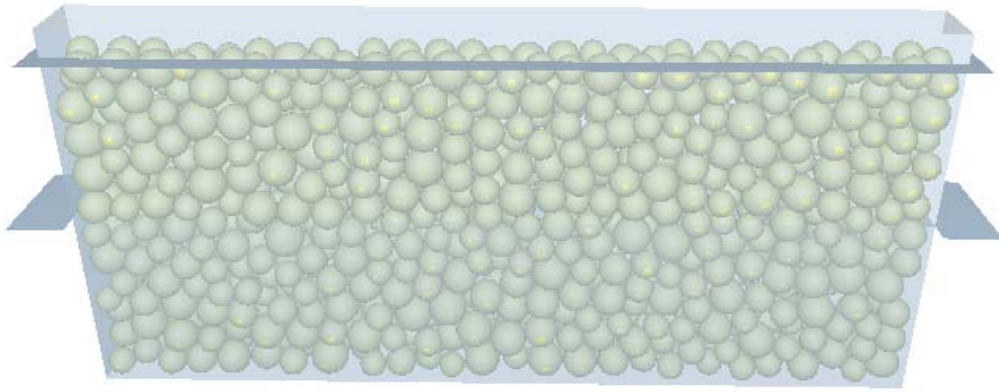
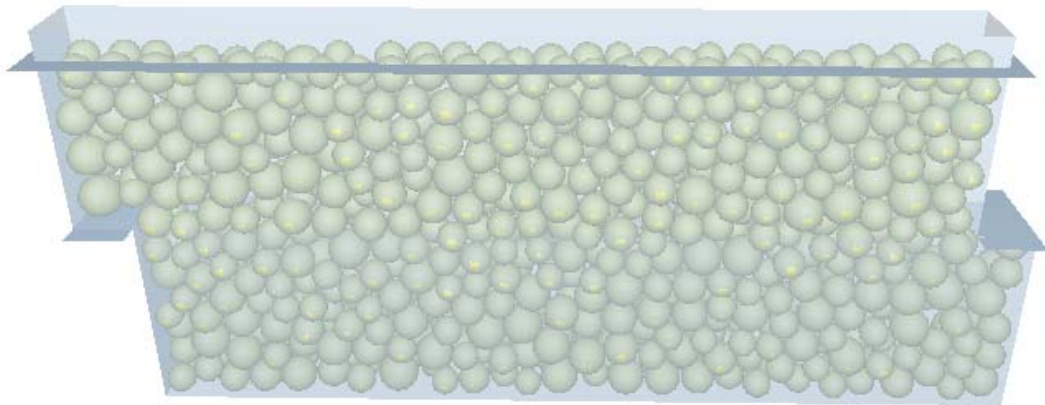


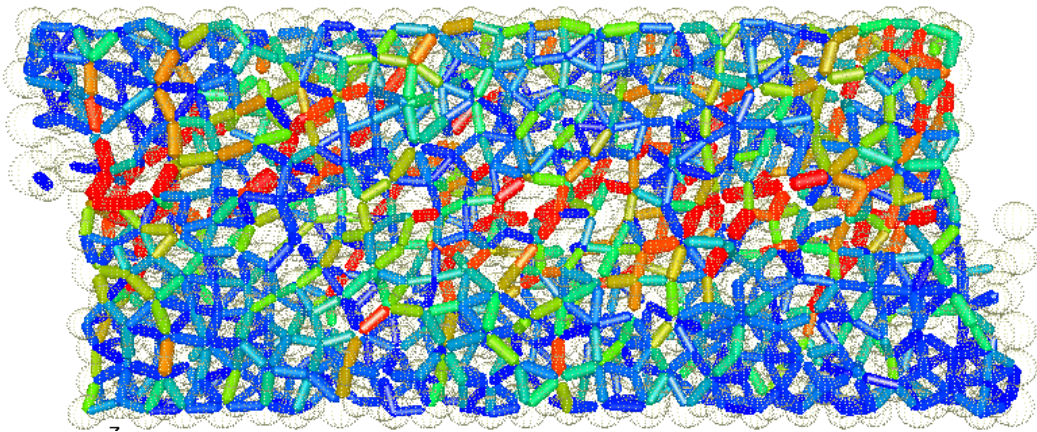
Figure 3.8 Graphics of shear to normal force ratio during direct shear test



(a) Normal force is applied



(b) End of the test



(c) Contact force illustration at the final stage

Figure 3.9 Direct shear test simulation

3.4 Bearing Capacity Calculation Models

The outline of the bearing capacity problem is shown in Figure 3.10. This problem is analyzed by the analytical methods, finite element method and discrete element method, respectively and then the results are compared.

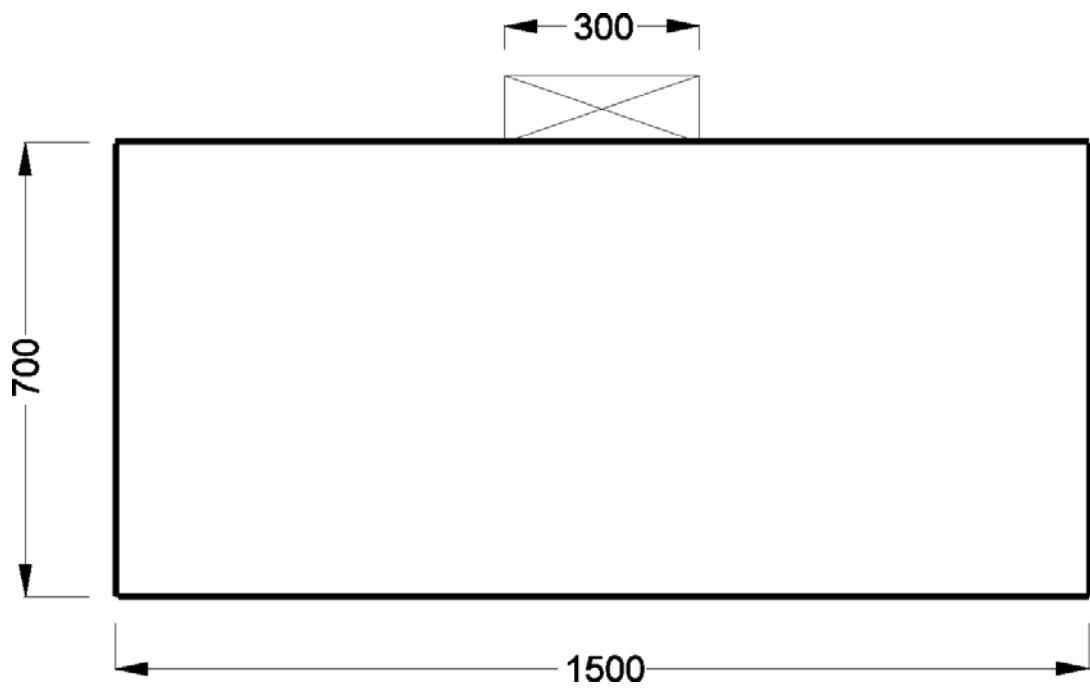


Figure 3.10 Bearing capacity model dimensions

3.4.1 Bearing Capacity From Analytical Methods

There are several analytical methods to compute the bearing capacity of shallow foundations. But the most common methods are Terzaghi, Meyerhof, Hansen and Vesic bearing capacity formulations (Bowles, 1996). The general form of all these methods is:

$$q_{ult} = c \cdot N_c \cdot f_c + q \cdot N_q \cdot f_q + 0.5 \cdot B \cdot \gamma \cdot N_\gamma \cdot f_\gamma \quad (3.6)$$

where,

q_{ult} : ultimate bearing capacity

c : cohesion of soil

q : surcharge at foundation depth

B : minimum width of footing

γ : unit weight of soil

N_c, N_q, N_γ : dimensionless bearing capacity factors

f_c, f_q, f_γ : dimensionless correction factors for shape, inclination, eccentricity, etc.

In our model, there is no cohesion in the soil and foundation depth is zero. Therefore, “ c ” and “ q ” terms vanish in the equation 3.6. Additionally, f_γ is unity for strip footings without inclination and eccentricity. Therefore, the equation 3.6 simplifies to:

$$q_{ult} = 0.5 \cdot B \cdot \gamma \cdot N_\gamma \quad (3.7)$$

The complete list of N_γ term for different bearing capacity methods are given in Table 3.5 (Bowles, 1996). Since the internal friction angle is estimated as 33° for our problem, the bearing capacity factors N_γ are;

Terzaghi $N_\gamma = 32.0$

Meyerhof $N_\gamma = 26.6$

Hansen $N_\gamma = 24.8$

Vesic $N_\gamma = 35.6$

Table 3.5 List of N_γ term for the bearing capacity formulations

ϕ	Terzaghi	Meyerhof	Hansen	Vesic
0	0.00	0.00	0.00	0.00
2	0.20	0.01	0.01	0.15
4	0.40	0.04	0.05	0.34
6	0.60	0.11	0.11	0.57
8	0.90	0.21	0.22	0.86
10	1.20	0.37	0.39	1.22
12	1.70	0.60	0.63	1.69
14	2.30	0.92	0.97	2.29
16	3.00	1.37	1.43	3.06
18	3.90	2.00	2.08	4.07
20	4.90	2.87	2.95	5.39
22	5.80	4.07	4.13	7.13
24	7.80	5.72	5.75	9.44
26	11.70	8.00	7.94	12.54
28	15.70	11.19	10.94	16.72
30	19.70	15.67	15.07	22.40
32	27.90	22.02	20.79	30.21
34	36.00	31.15	28.77	41.06
36	52.00	44.43	40.05	56.31
38	80.00	64.07	56.17	78.02
40	100.40	93.69	79.54	109.41
42	180.00	139.32	113.95	155.54
44	257.00	211.41	165.58	224.63

In our model,

$B = 0.3 \text{ m}$ (Figure 3.10)

$\gamma = 134.5 \text{ kN/m}^3$ (Table 3.2)

Therefore, the ultimate bearing capacities from analytical methods are:

Terzaghi $q_{ult} = 646 \text{ kPa}$

Meyerhof $q_{ult} = 537 \text{ kPa}$

Hansen $q_{ult} = 500 \text{ kPa}$

Vesic $q_{ult} = 718 \text{ kPa}$

3.4.2 Numerical Analysis of Bearing Capacity by FEM

For the numerical analysis of the bearing capacity, plane strain FEM software, Phase² is used. The model geometry is exactly the same as the DEM model. The geometry and input parameters are given in Figure 3.11 and Table 3.6, respectively.

The analysis procedure is as follows:

- Model outline is prepared as shown in Figure 3.11.
- Elastic and yield parameters obtained from the calibration runs are introduced to the model as in Table 3.6. To investigate effect of dilation angle to the results, model is analyzed with different dilation angles 0° (non-dilant flow), 5°, 10° and 33° (associated flow), respectively.
- In order to see post failure behavior, the prescribed displacement applied to the footing. The displacement is increased in 10 stages and the vertical stress beneath the footing is recorded.

The obtained model results are illustrated in Figure 3.12 and Figure 3.13, respectively.

Table 3.6 Model parameters for FEM analysis of bearing capacity

Modulus of Elasticity	6 300 kPa
Poisson's Ratio	0.38
Yield Criterion	Mohr-Coulomb
Internal Friction Angle	33°
Cohesion	0
Dilation Angle	0°, 5°, 10°, 33°

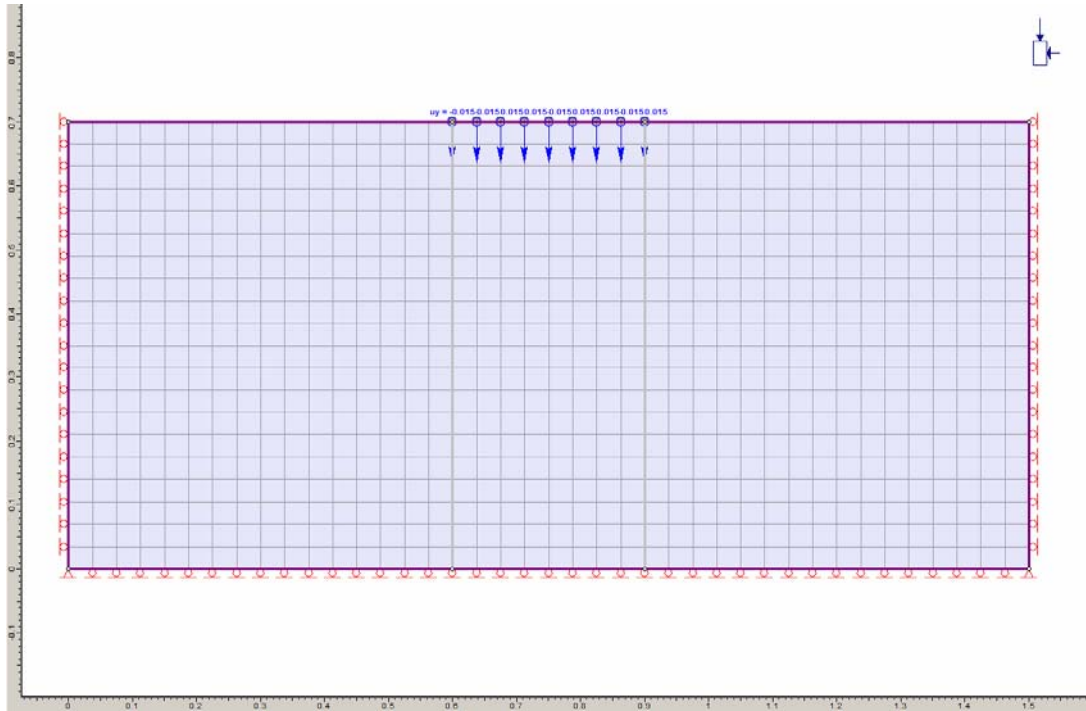


Figure 3.11 Phase² model of bearing capacity analysis

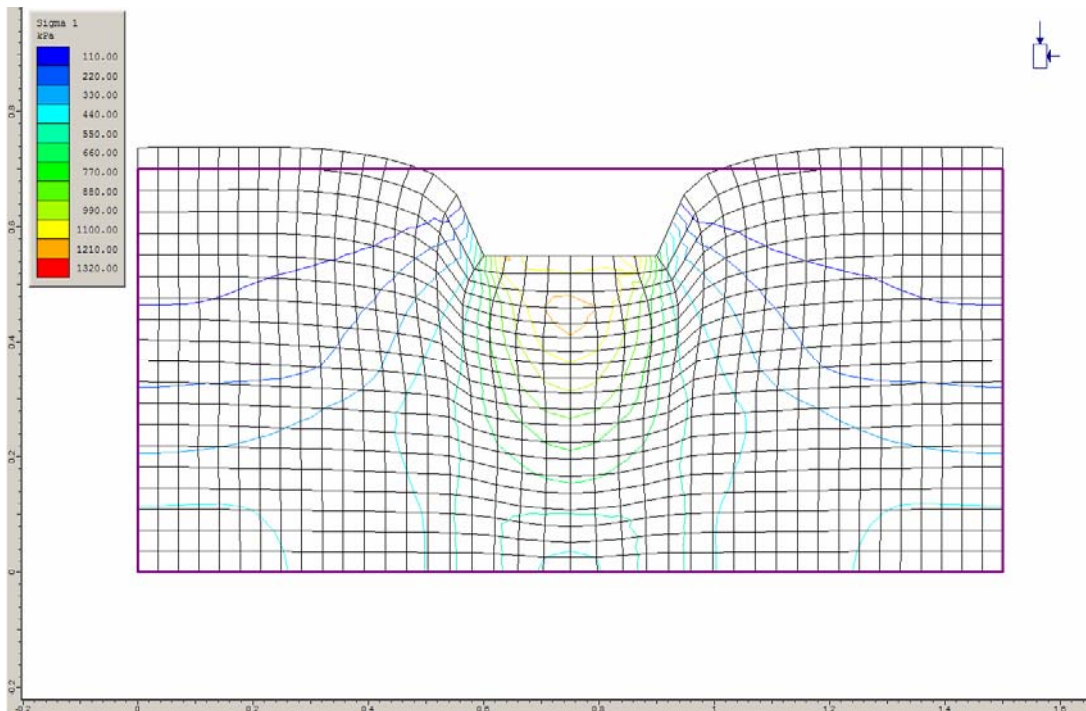


Figure 3.12 Indication of major principal stress on deformed shape of the FEM model at 0.15 m settlement of footing (True scale at $\psi=0^\circ$)

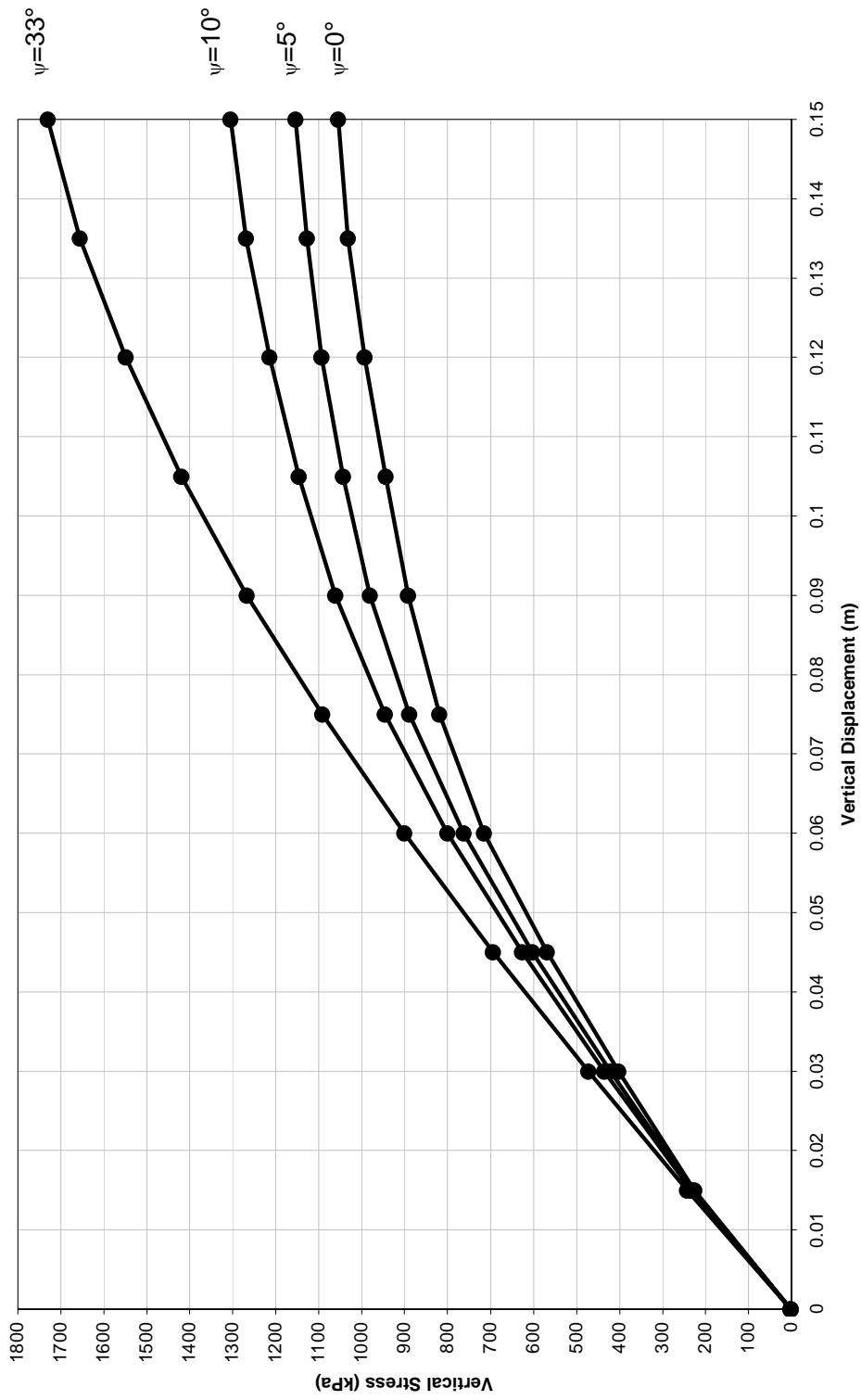


Figure 3.13 Displacement versus vertical stress diagram from FEM analysis

3.4.3 Numerical Analysis of Bearing Capacity by DEM

The procedure for DEM analysis of the problem is given below:

- A rigid block representing the footing is placed to the previously generated particle model. Model is bounded by rigid walls and gravity is maintained.
- Footing is started to be pushed down while measuring the vertical component of contact forces beneath the footing. Then, the average stress is obtained by dividing the total contact forces to the footing area.

The visual representation of the progress of simulations and the result of analysis are given in Figure 3.14 and Figure 3.15, respectively.

The comparison of the results obtained from all analysis performed in this thesis is indicated in Figure 3.16.

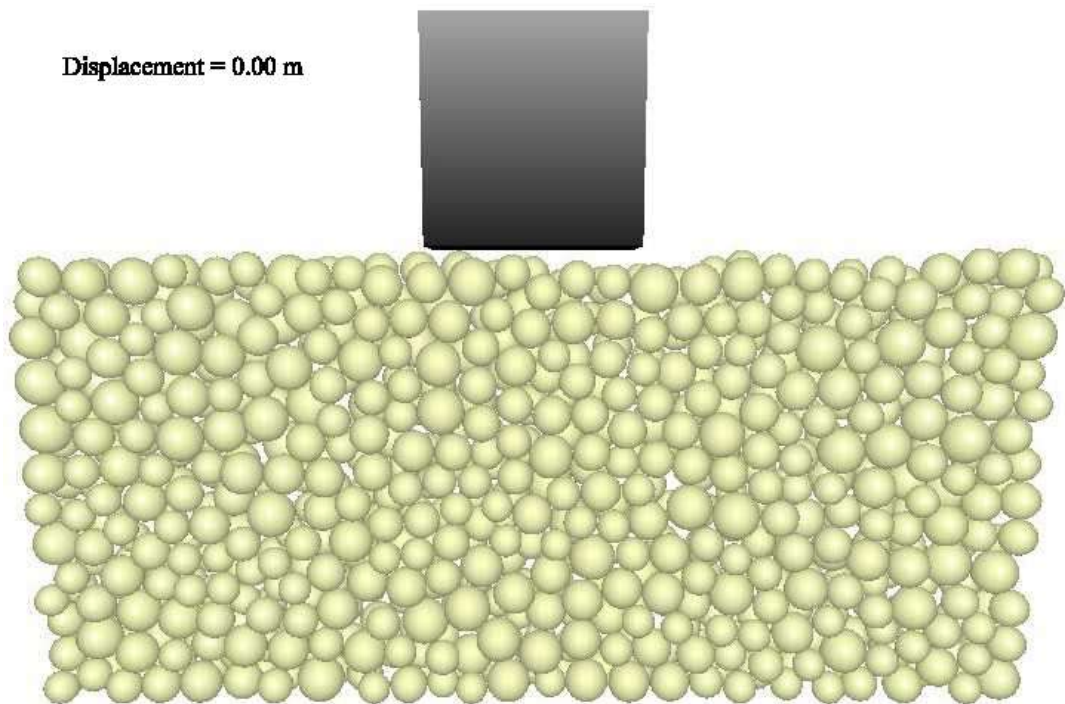
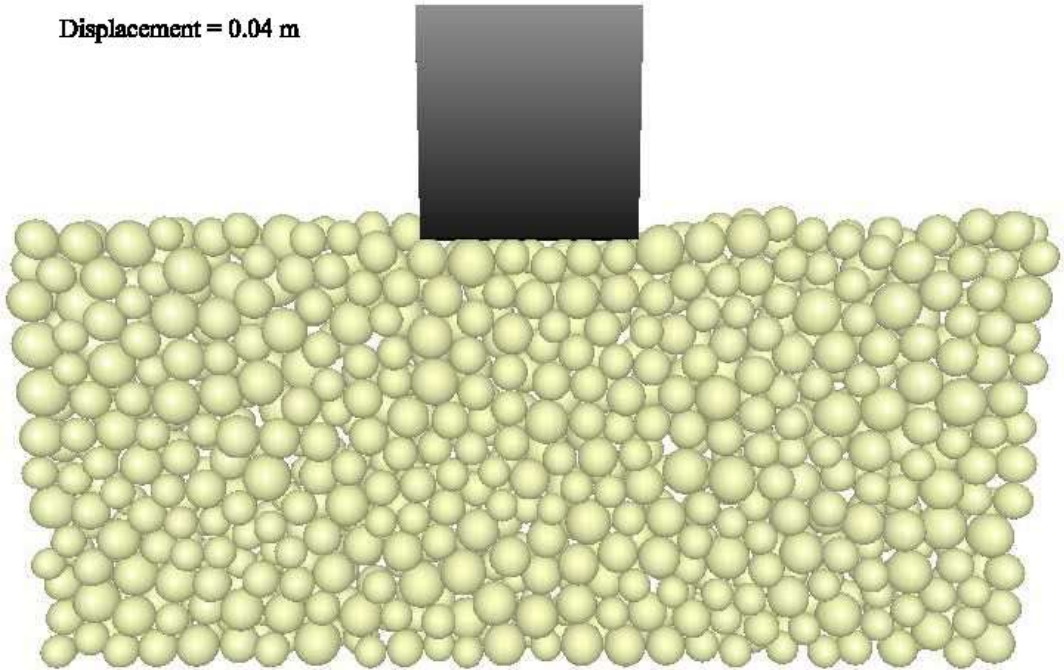


Figure 3.14 The Progress of bearing capacity failure in time

Displacement = 0.04 m



Displacement = 0.06 m

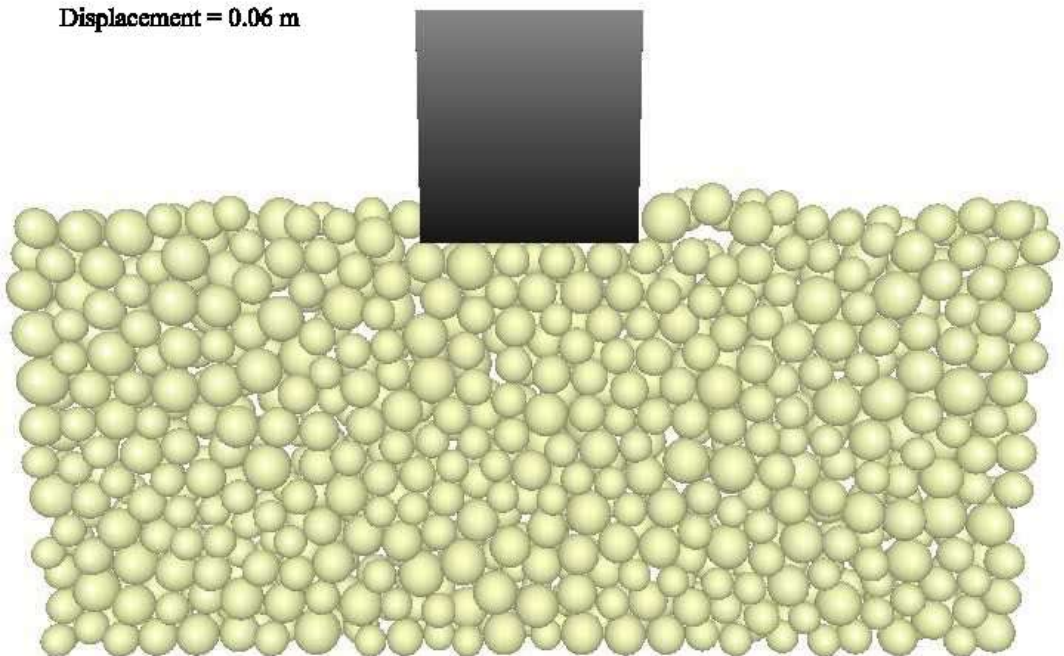
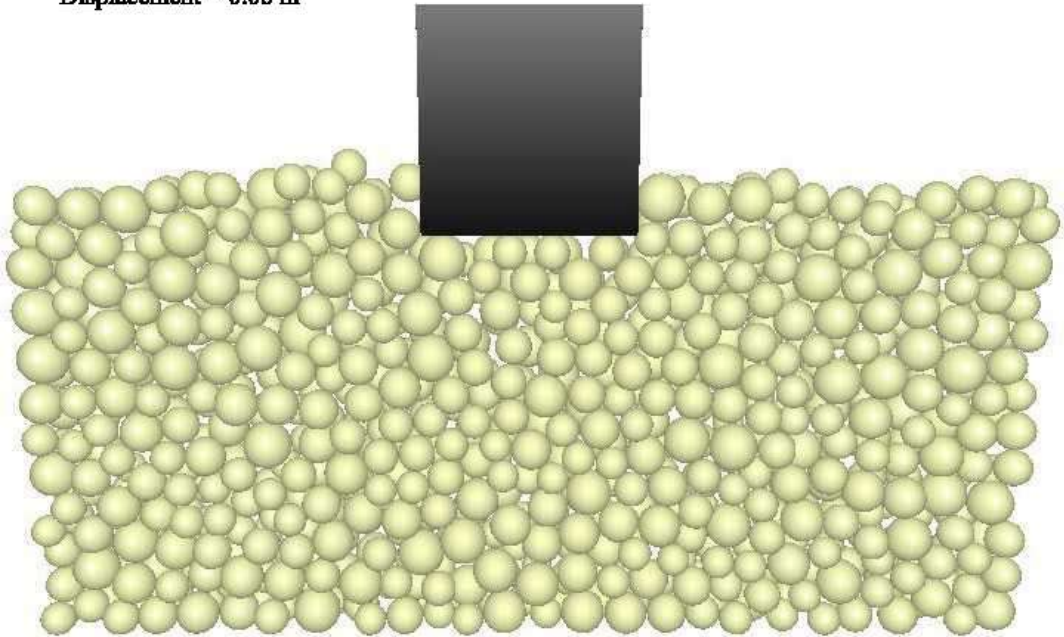


Figure 3.14 (cont'd)

Displacement = 0.08 m



Displacement = 0.10 m

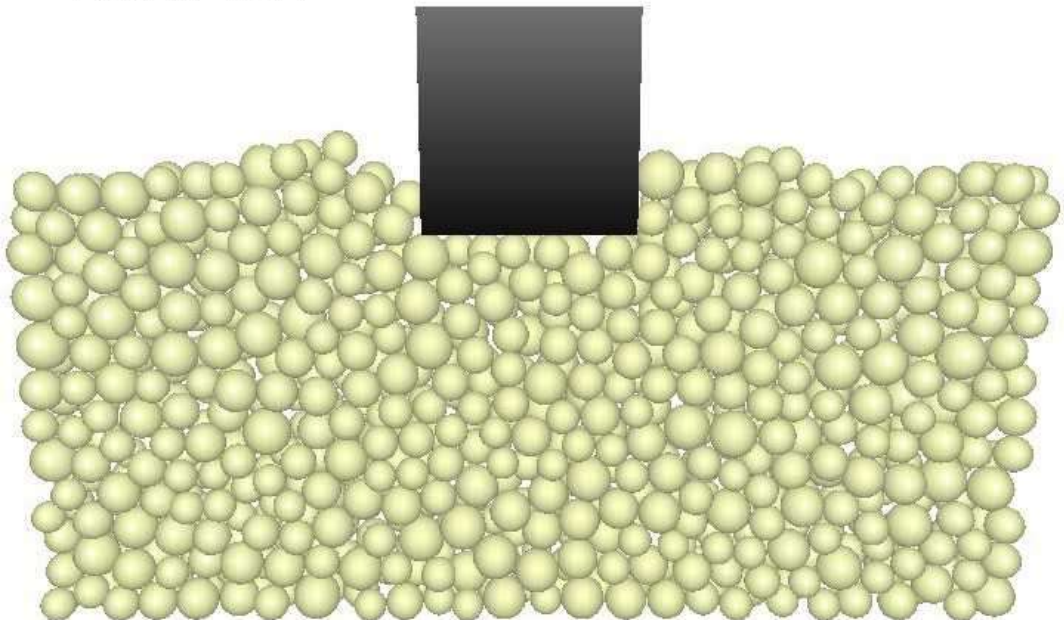


Figure 3.14 (cont'd)

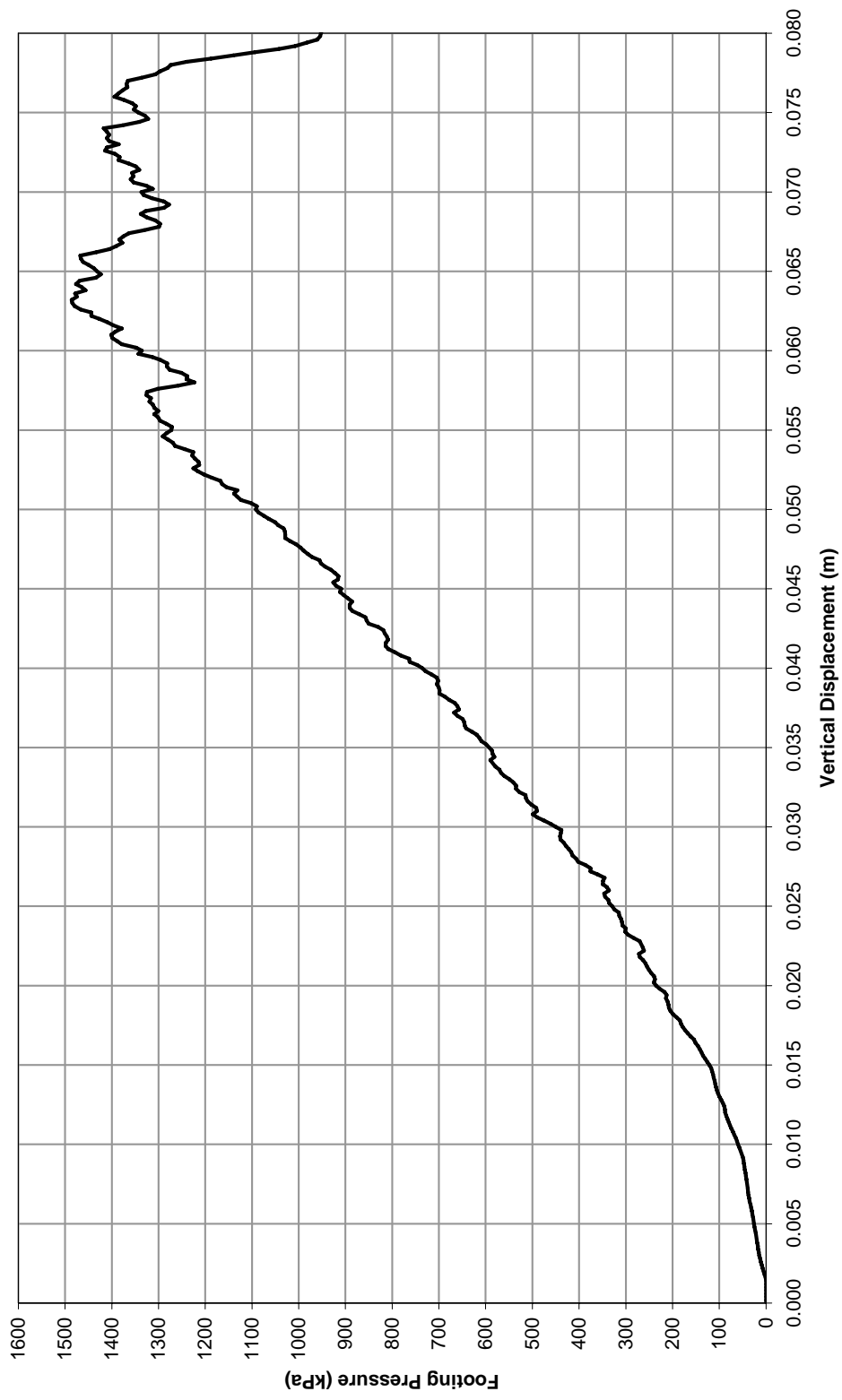


Figure 3.15 Displacement versus footing pressure diagram from DEM analysis

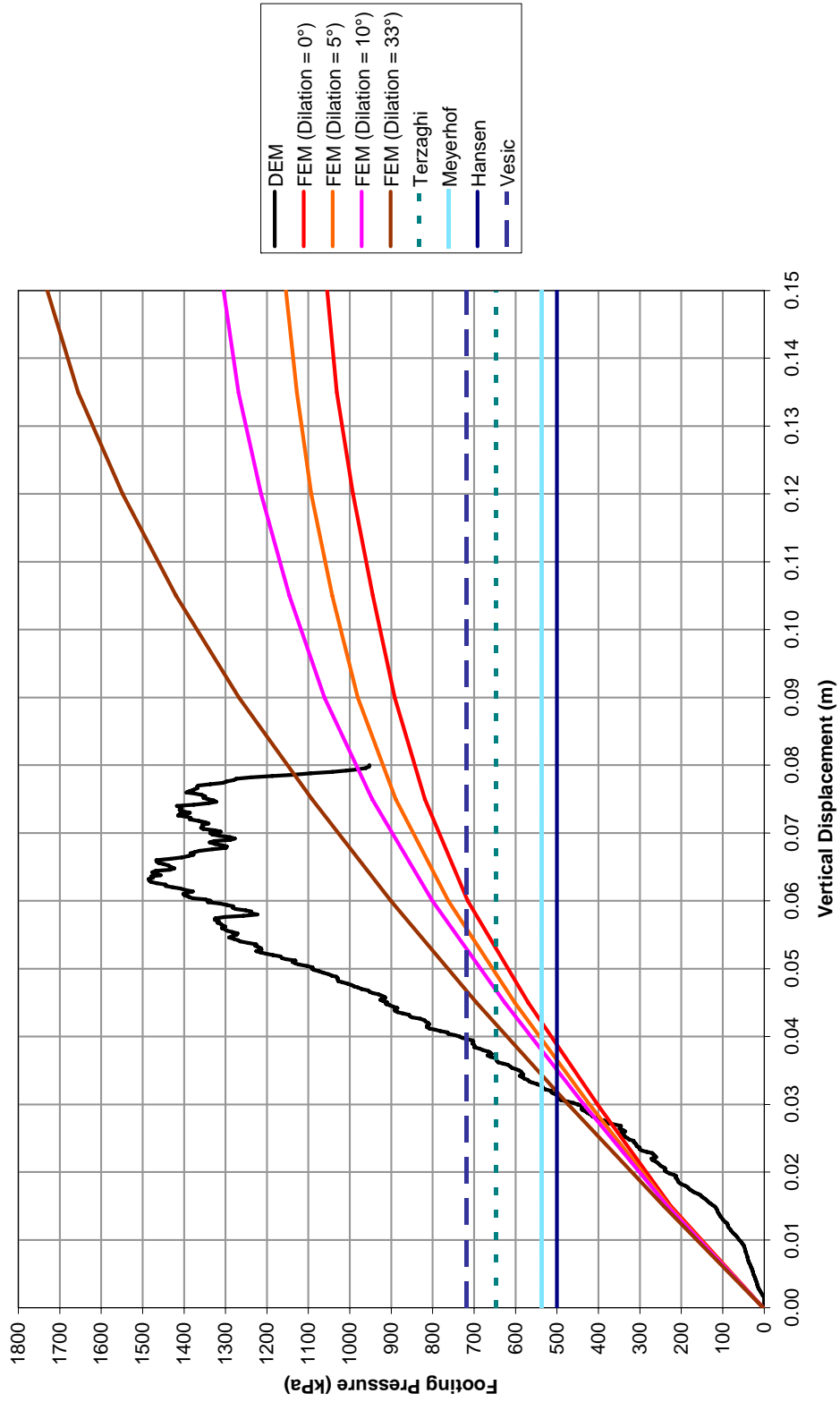


Figure 3.16 Comparison of bearing capacity calculations

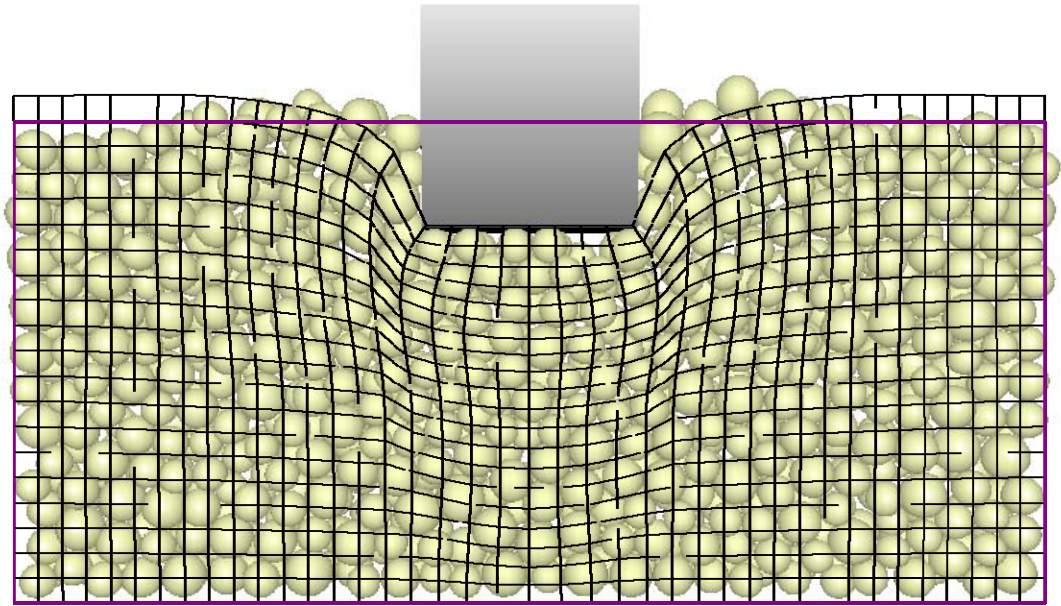


Figure 3.17 Comparison of deformed shape of FEM and DEM as of 0.15 m settlement

CHAPTER 4

DISCUSSION OF RESULTS AND CONCLUSIONS

In this study, following a general presentation of the Discrete Element Method (DEM), its performance is investigated in the numerical analysis of bearing capacity problems. For the comparison purposes, the bearing capacity model utilized for DEM analyses is also tested by analytical and finite element solutions.

The material parameters required for DEM analysis is radically different from other alternative methods based on continuum assumption. Those parameters are micro-mechanical parameters that define the behavior of a single particle (spherical in this case). Obviously, macro-mechanical properties of the assembly formed by randomly placed particles are required for comparisons. Hence, two different sets of calibration tests are performed to achieve elastic and plastic properties of the assembly. It should be noted that the particle size utilized in discrete element models are quite coarse and unrealistically far from the particle size range of real soils.

First, isotropic compression test is conducted to measure elastic properties of the formed assembly. It is observed that the similar Poisson's ratios are measured under different loadings, while tangent modulus of elasticity is increasing with increasing axial strain. However, modulus of elasticity tends to decrease in higher axial strain in real materials. This phenomenon can be attributed to the loose state of the assembly, since its unit weight is about 13.5 kN/m^3 , which is much lower than any real soil. Under higher loads, greater tangential modulus of elasticity and lower Poisson's ratio would be expected. Practically, elastic properties do not have much significance in calculation of ultimate bearing capacity, if the displacement is not a concern. As a result of isotropic compression test, modulus of elasticity (E) of 6300 kPa and Poisson's ratio (ν) of 0.38 are obtained for the tested assembly.

Then, the only yield parameter, which is the internal friction angle (ϕ), in this case, is acquired by direct shear test simulation. Due to the restrictions of the DEM software, constant volume shear box test is carried out. The normal force is observed to increase during shear, that is to say, the material tends to dilate. Additionally, despite the fact that the particles are spherical and that the inter-particle friction coefficient is 0.5, T to N ratio of 0.65 corresponding to $\phi = 33^\circ$ is measured during the test. This means that the interlocking of particles dominates the shear behavior of the assembly and this result also supports the dilative property.

After determining the macro-mechanical properties, the DEM, FEM and analytical analyses of bearing capacity problem are performed and the results are compared. The bearing capacity failure in DEM analysis occurs at a relatively lower level of foundation displacement. This result shows that the modulus of elasticity is actually higher than that obtained from the results of isotropic compression test. However, the ultimate bearing capacities are in quite acceptable tolerance. It is also realized that the associated flow rule causes extreme overestimation of bearing capacity and large displacements.

On the other hand, the ultimate bearing capacities obtained from the numerical analyses are, in general, 1.5 to 2 times higher than the analytical results. A possible reason for this is that the boundaries in the numerical analyses are too close to the focused area. Moreover, it is acknowledged that the analytical bearing capacity formulations generally under estimate the ultimate bearing capacity for granular soils with high friction angle (Lambe and Whitman, 1976, Bowles, 1996 and Zadroga, 1994). Zadroga (1994) investigated this phenomenon through model tests and proposed a different calculation approach for the bearing capacity of non-cohesive soils. It is obvious that the numerical methods and theoretical methods have different constitutive assumptions. Theoretical methods assume the soil as perfectly rigid and they do not consider the displacements or compressibility of soil (Vesic, 1973). Additionally, unlike the other two terms in the analytical bearing capacity expression, there is no closed form solution of N_γ and many different approximations exist, which reflect the theoretical uncertainty associated with this term. Griffith (1982) indicated that N_γ is inversely proportional to the footing width

and influence of the footing size increases with increasing angle of friction in finite elements. That is why, the model test results differ from the analytical solutions for cohesionless soils (Bowles, 1996).

Consequently, although the DEM is a relatively new method and requires excessive calculation time for the current technology, it is really a promising numerical analysis technique in geomechanical application, like bearing capacity problems.

At the end of this study, it would be appropriate to draw a road map and recommend further studies regarding DEM in geomechanics:

- The major shortcoming of this method is the requirement of extreme computation time due to contact detection. Therefore, faster, more efficient contact detection algorithms should be developed.
- Greater attention should be paid to the development of parallel processing techniques by which the power of multi-processors (and/or computers) can be combined.
- Different time stabilization techniques should be studied. Implicit solution methods may be applicable as alternatives for static analyses.
- The DEM method can be coupled with other numerical analysis techniques like FEM. Therefore, the soil-structure interaction problems can be handled more precisely.
- Fluid-DEM coupled analysis should be investigated to model undrained condition of the soil and to analyze the liquefaction problems.
- The studies should be focused on the homogenization methods so that continuum based methods can be bridged to discrete methods.
- The DEM should be validated on several other geotechnical problems as well.

REFERENCES

- ABAQUS Inc. (2004) *Documentation of ABAQUS v6.5*
- Alonso-Marroquin, F. (2004) Micromechanical Investigation of Soil Deformation: Incremental Response and Granular Ratcheting, *Thesis*, University of Stuttgart
- Alonso-Marroquin, F. and Herrmann, H.J. (2005) *The Incremental Response of Soils. An Investigation Using a Discrete-Element Model*, *Journal of Engineering Mathematics*, 52: 11-34
- Anandarajah, A. (1994). Discrete-Element Method for Simulating Behavior of Cohesive Soil, *Journal of Geotechnical Engineering* 120(9), 1593-1613
- Bardet, J.P. and Proubet, J. (1991) Adaptive Dynamic Relaxation for Statics of Granular Materials, *Computers & Structures*; 39(3/4), 221-229
- Bowles, J.E. (1996) *Foundation Analysis and Design* 5th Edition, The McGraw-Hill Companies, Inc., ISBN 0-07-912247-7
- Cambou, B., Dubujet, P., Emeriault, F. and Sidoroff, F. (1995) Homogenization for Granular Materials, *European Journal of Mechanics A/Solis*, 14(2), 255-276
- Calvetti, F., Viggiani, G. and Tamagnini, C. (2003) Micromechanical inspection of constitutive modeling, *Constitutive modelling and analysis of boundary value problems in Geotechnical Engineering*, Benevento, 187-216
- Cheng, Y.P., Nakata, Y. and Bolton, M.D. (2003) Discrete Element Simulation of Crushable Soil, *Geotechnique*, 53(7), 633-641
- Cundall, P.A. (1971). A Computer Program for Simulating Progressive, Large-Scale Movements in Blocky Rock Systems, *Proceedings of the Symposium of the International Society of Rock Mechanics*, Vol.: 1 Paper no.: II-8, Nancy France
- Cundall, P.A. (1988) Formulation of a Three-dimensional Distinct Element Model – Part I A Scheme to Detect and Represent Contacts in a System Composed of Many Polyhedral Blocks, *International Journal of Rock Mechanics and Mineral Sciences & Geomechanical Abstracts*, 25(3), 107-116
- Cundall, P.A. (2001) A Discontinuous Future for Numerical Modelling in Geomechanics, *Proceedings of the Institution of Civil Engineers, Geotechnical Engineering*, 149(1), 41-47

- Cundall, P.A. and Hart, R.D. (1992) Numerical Modeling of Discontinua, *Journal of Engineering Computation*, 9, 101-113
- Cundall, P.A. and Strack, O.D.L. (1979) A Discrete Numerical Model for Granular Assemblies, *Geotechnique* 29(1), 47-65
- D'Addetta, G.A. (2004). Discrete Models for Cohesive Frictional Materials, *PhD. Thesis*, University of Stuttgart
- D'Addetta, G.A. and Ramm, E. (2005) A Particle Model for Cohesive Frictional Materials, *5th GRACM International Congress on Computational Mechanics*, Limassol
- Deluzarche, R. And Cambou, B. (2006) Discrete Numerical Modelling of Rockfill Dams, *International Journal for Numerical and Analytical Methods in Geomechanics*, Early View (in press)
- DEM Solutions (2006) *Documentation of EDEM*
- Dinesh, S.V. and Sitharam, T.G. (2003) Discrete Element Simulation of Liquefaction Behavior of Granular Soils under Cyclic Loading, *CPFTEGE*
- Emeriault, F., Cambou, B. and Mahboubi A. (1996) Homogenization for Granular Materials: non Reversible Behaviour, *Mechanics of Cohesive-Frictional Materials*, 1, 199-218
- Favier, J.F., Abbaspour-Fard, M.H., Raji, A.O. and Kremmer, M. (1999) Shape Representation of Axi –Symmetrical Arbitrary Particles in Discrete Element Simulation Using Multi-Element Model Particles, *Engineering Computations*, 16(4), 467-480
- Griffiths, D.V. (1982) Computation of Bearing Capacity Factors Using Finite Elements, *Geotechnique* , 32(3), 195-202
- Hart, R.D, Cundall P.A. and Lemos J. (1988) Formulation of a Three-dimensional Distinct Element Model – Part II Mechanical Calculation of Motion and Interaction of a System Composed of Many Polyhedral Blocks, *International Journal of Rock Mechanics and Mineral Sciences & Geomechanical Abstracts*, 25(3), 117-125
- Hibbeler, R.C. (1989) *Engineering Mechanics – Dynamics 5th Edition*, Macmillan Publishing Company, ISBN 0-02-946093-X
- Hentz, S., Daudeville, L. and Donzé F.V.(2002) Discrete Element Modelling of Concrete and Identification of the Constitutive Behaviour, *15th ASCE Engineering Mechanics Conference*, Columbia University, NY

- Itasca Consulting Group (2006) *Online Manual of PFC^{2D} 3.1 Particle Flow Code in Two Dimensions*, Itasca Consulting Group Inc., Minneapolis
- Itasca Consulting Group (2006) *Online Manual of PFC^{3D} 3.1 Particle Flow Code in Three Dimensions*, Itasca Consulting Group Inc., Minneapolis
- Jiang, M.J., Yu, H.-S. and Harris D. (2005) Discrete Element Modelling of Deep Penetration in Granular Soils, *International Journal for Numerical and Analytical Methods in Geomechanics*, 30, 335-361
- Lambe, T.W. and Whitman, R.V. (1979) *Soil Mechanics, SI Version*, John Wiley & Sons, Inc., ISBN 0-471-02261-6
- Magnier, S.A. and Donze, F.V. (1998) Numerical Simulations of Impacts Using a Discrete Element Method, *Mechanics of Cohesive-Frictional Materials*, 3, 257-276
- Masson, S. and Martinez, J. (2001) Micromechanical Analysis of the Shear Behavior of a Granular Material, *Journal of Engineering Mechanics*, 127(10), 1007-1016
- Maynar, M.J.M. and Rodriguez, L.E.M. (2005) Discrete Numerical Model for Analysis of Earth Pressure Balance Tunnel Excavation, *Journal of Geotechnical and Geoenvironmental Engineering*, 131(10), 1234-1242
- Mohammadi, S. (2003) *Discontinuum Mechanics Using Finite and Discrete Elements*, WIT Press Southampton, Boston, ISBN 1-85312-959-3
- Munjiza, A. (2004). *The Combined Finite-Discrete Element Method*, John Wiley & Sons, Ltd., ISBN 0-470-84199-0
- Nezami, E.G., Hashash, Y.M.A., Zhao, D. and Ghaboussi, J. (2004) A Fast Contact Detection Algorithm for 3-D Discrete Element Method, *Computers and Geotechnics*, 31, 575-587
- Nezami, E.G., Hashash, Y.M.A., Zhao, D. and Ghaboussi J. (2006) Shortest Link Method for Contact Detection in Discrete Element Method, *International Journal for Numerical and Analytical Methods in Geomechanics*, 30, 783-801
- Ng, T.-T. (1992) The Elliptic Discrete Element Method as a New Approach To Simulating Granular Media, *Proceedings of Asian Pacific Conference on Computational Mechanics*, Hong Kong
- Ng, T.-T. (2006) Input Parameters of Discrete Element Methods, *Journal of Engineering Mechanics*, 132(2), 723-729

- O'Sullivan, C.; Bray, J.D. and Li, S. (2003) A New Approach for Calculating Strain for Particulate Media, *International Journal for Numerical and Analytical Methods in Geomechanics*, 27, 859-877
- O'Sullivan, C.; Bray, J.D. and Riemer, M.F. (2002) Influence of Particle Shape and Surface Friction Variability on Response of Rod-Shaped Particulate Media, *Journal of Engineering Mechanics*; 128(11), 1182-1192
- Potyondya, D.O. and Cundall, P.A. (2004) A Bonded-Particle Model for Rock, *International Journal of Rock Mechanics & Mining Sciences*, 41, 1329-1364
- Sallam, A.M. (2004). Studies on Modeling Angular Soil Particles Using the Discrete Element Method, *PhD. Thesis*, University of South Florida
- Shamy, U.E. and Zeghal, M. (2005) Coupled Continuum-Discrete Model for Saturated Granular Soils, *Journal of Engineering Mechanics*, 131(4), 413-426
- Shimizu, Y. and Cundall, P.A. (2001) Three-Dimensional DEM Simulations of Bulk Handling by Screw Conveyors, *Journal of Engineering Mechanics*, 127(9), 864-872
- Sitharam, T.G. (2000) Numerical Simulation of Particulate Materials Using Discrete Element Modelling, *Current Science*, 78(7), 876-886
- Van Baars, S. (1996) Discrete Element Analysis of Granular Materials, *Dissertation*, University of Technology Delft
- Vesic, A.S. (1973) Analysis of ultimate loads of shallow foundations, *Journal of Soil Mechanics and Foundation*, ASCE, 99(1), 45-73
- Yao, M. and Anandarajah, A. (2003) Three-Dimensional Discrete Element Method of Analysis of Clays, *Journal of Engineering Mechanics*, 129(6), 585-596
- Zadroga, B. (1994) Bearing Capacity of Shallow Foundations on Noncohesive Soils, *Journal of Geotechnical Engineering*, ASCE, 120(11), 1991-2008
- Zhang, L. and Thornton, C. (2002) DEM Simulation of Direct Shear Test, *15th ASCE Engineering Mechanics Conference*, Columbia University, New York